Synthesis, Characterization, and *X*-Ray Crystal Structures† of Mononuclear Copper(II) Complexes with Unsymmetrical Quadridentate Ligands involving an Imidazole Moiety and Discrete Imidazolate-bridged Binuclear Copper(II) Complexes with Non-identical Co-ordination Geometries in the Binuclear Unit

Naohide Matsumoto,* Toshifumi Akui, Hiroyuki Murakami, Junko Kanesaka, and Akira Ohyoshi
Department of Applied Chemistry, Faculty of Engineering, Kumamoto University, Kurokami 2-39-1, Kumamoto 860, Japan
Hisashi Ōkawa
Department of Chemistry, Faculty of Science, Kyushu University, Hakozaki, Higashi-ku, Fukuoka 812, Japan

Mononuclear copper(II) complexes with unsymmetrical quadridentate Schiff bases involving an imidazole moiety $[Cu(HL^1)][ClO_4]$ (**1**) and $[Cu(HL^2)][ClO_4]$ (**2**) have been prepared and characterized, where H_2L^1 denotes the 1 : 1 : 1 condensation product of acetylacetone, ethylenediamine, and 4-formylimidazole and H_2L^2 denotes that of acetylacetone, propane-1,3-diamine, and 4-formylimidazole. The structure of the unsymmetrical quadridentate ligand has been established by the ^1H n.m.r. spectrum of $[Ni(HL^1)][ClO_4]$. The deprotonated complex $[Cu(L^1)]$, which can function as ligand at the imidazolate nitrogen, has been isolated and characterized. *X*-Ray crystal structures of complexes (**1**) and (**2**) have been determined. Complex (**1**) crystallizes in the monoclinic space group $P2_1/n$ with $a = 22.146(2)$, $b = 9.659(1)$, $c = 7.126(1)$ Å, $\beta = 98.35(1)°$, and $Z = 4$. Complex (**2**) crystallizes in the triclinic space group $P\bar{1}$ with $a = 10.551(4)$, $b = 11.602(3)$, $c = 7.307(1)$ Å, $\alpha = 98.95(1)°$, $\beta = 96.99(2)$, $\gamma = 113.04(2)°$, and $Z = 2$. In both complexes (**1**) and (**2**), the copper(II) atom assumes a square-planar co-ordination environment with N_3O donor atoms of unsymmetrical quadridentate ligands. Two imidazolate-bridged binuclear copper(II) complexes $[Cu(L^1)Cu(tfacac)_2]$ (**3**) (tfacac = trifluoroacetylacetonate) and $[Cu(L^1)Cu(tebima)][PF_6][ClO_4]\cdot Me_2CO$ (**4**) {tebima = tris[2-(*N*-ethylbenzimidazolyl)methyl]amine} have been prepared by the reaction of (**1**) (as a-site component complex) and $[Cu(tfacac)_2]$ or $[Cu(tebima)][ClO_4]_2\cdot 2H_2O$, exhibiting an unsaturated co-ordination site (b-site component complex), in the presence of one equivalent of triethylamine. Complexes (**3**) and (**4**) have been characterized by elemental analyses, melting points, molar electrical conductivities, i.r., electronic, and e.s.r. spectra, magnetic susceptibilities, and single-crystal *X*-ray diffraction. Complex (**3**) crystallizes in the triclinic space group $P\bar{1}$ with $a = 11.462(4)$, $b = 16.708(8)$, $c = 7.692(2)$ Å, $\alpha = 93.96(3)$, $\beta = 109.98(2)$, $\gamma = 71.74(3)°$, and $Z = 2$. Complex (**4**) crystallizes in the triclinic space group $P\bar{1}$ with $a = 13.131(5)$, $b = 19.285(6)$, $c = 10.878(4)$ Å, $\alpha = 93.89(2)$, $\beta = 92.83(2)$, $\gamma = 114.64(2)°$, and $Z = 2$. The *X*-ray structural analyses of (**3**) and (**4**) verify the discrete imidazolate-bridged binuclear structures in which the two co-ordination geometries in the binuclear unit are non-identical. In the complex (**3**), one copper atom has a square-planar co-ordination geometry and the other has a square-based pyramidal co-ordination geometry. In (**4**), one copper atom has a square-planar co-ordination geometry and the other a geometry intermediate between square-based pyramidal and trigonal bipyramidal. The Cu–N(imidazolate) bond distances are 1.966(3) Å for (**3**) and 1.957(8) Å for (**4**). The magnetic susceptibility data gave the antiferromagnetic interaction parameters $2J = -112$ cm^{-1} for (**3**) and -140 cm^{-1} for (**4**). The e.s.r. spectra of complexes (**3**) and (**4**) measured in frozen solutions (77 K) at *X*-band frequency showed broad $\Delta M = 1$ and weak $\Delta M = 2$ absorptions.

Discrete imidazolate-bridged metal complexes are of current interest, since an imidazolate-bridged copper(II)–zinc(II) centre has been discovered in bovine erythrocyte superoxide dismutase (besod)[1] and an imidazolate-bridged copper(II)–iron(III) centre has been postulated in cytochrome c oxidase.[2] Synthesis and characterization of synthetic model compounds of besod and cytochrome c oxidase is therefore desirable. The structural characteristics to be satisfied as model compounds of besod and cytochrome c oxidase can be summarised as follows: (i) the discrete binuclear complex contains an imidazolate bridge; (ii) the two co-ordination geometries in the binuclear unit are not identical; (iii) the two metal ions in the binuclear unit are different. A number of imidazolate-bridged metal complexes have been synthesized and characterized.[3,4] However, in most cases the metal ions are both copper(II) and the two co-ordination spheres in the binuclear unit are identical. In order to develop a synthetic route for the model compounds, a metal complex with an unsymmetrical quadridentate ligand involving an imidazole moiety is a key compound, because it is expected that such a compound reacts with a dissimilar second metal complex to produce discrete homo- and hetero-metal binuclear complexes as model compounds of the enzymes.

Therefore we have prepared and characterized two mononuclear copper(II) complexes (**1**) and (**2**), with unsymmetrical

† *Supplementary data available:* see Instructions for Authors, *J. Chem. Soc., Dalton Trans.*, 1988, Issue 1, pp. xvii—xx.

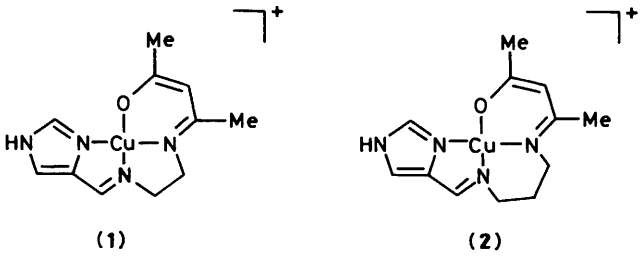

(1)

(2)

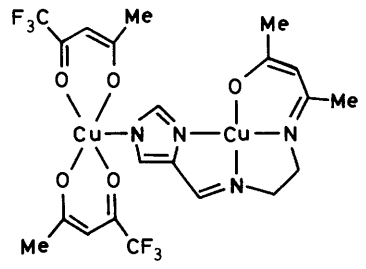

(3)

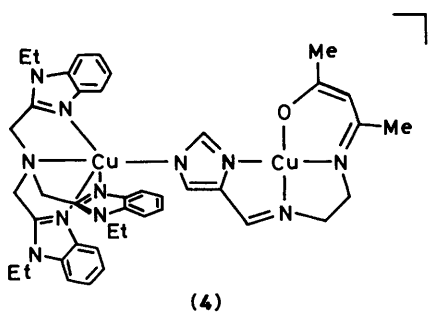

(4)

quadridentate ligands involving an imidazole moiety, as the key compounds. The deprotonated complex $[Cu(L^1)]$ which can function as the ligand at the imidazolate nitrogen to another metal ion has been prepared and characterized.

Two imidazolate-bridged binuclear copper(II) complexes (**3**) and (**4**) which satisfy structural characteristics (i) and (ii) described above have been prepared by the reaction of the copper(II) complex (**1**) and dissimilar second metal complexes bis(trifluoroacetylacetonato)copper(II), $[Cu(tfacac)_2]$, or {tris-[2-(*N*-ethylbenzimidazolyl)methyl]amine}copper(II) perchlorate, $[Cu(tebima)][ClO_4]_2$. In addition to the importance as model compounds of besod, these complexes allow the investigation of the magnetic interaction between two magnetic centres with non-identical co-ordination geometries through the imidazolate bridge. In this paper, the synthesis, characterization, magnetic properties, and *X*-ray structures of complexes (**3**) and (**4**) are described.

Experimental

Materials.—Starting materials were purchased from Tokyo Chemical Industry Co., Ltd. and used without further purification.

Synthesis of Mononuclear Copper(II) Complexes with Unsymmetrical Ligands involving an Imidazole Moiety (a-Site Component Complexes).—*4-Formylimidazole.* 4-(Hydroxymethyl)-imidazole hydrochloride was prepared according to the literature.[5] The hydrochloride salt was converted to the free base by neutralization with sodium carbonate[6] and the neutral base was oxidized to the aldehyde by the action of manganese dioxide in 1,4-dioxane at 80 °C.[7]

$[Cu(HL^1)][ClO_4]$ (**1**) (*a-site component complex*). The 1:1 condensation product of acetylacetone and ethylenediamine was prepared according to the method of Costes *et al.*[8] To a solution of ethylenediamine (0.6 g, 10 mmol) in chloroform (50 cm^3) was added dropwise a solution of acetylacetone (1.0 g, 10 mmol) in chloroform (50 cm^3) at ambient temperature. After the completion of addition, the solution was stirred for an additional 3 h and then chloroform was evaporated under reduced pressure. The resultant viscous oil was dissolved in methanol (50 cm^3) and 4-formylimidazole (0.96 g, 10 mmol) was mixed. The mixture was warmed at 50 °C for 1 h and cooled to ambient temperature. To the solution was added a solution of copper(II) perchlorate hexahydrate (3.7 g, 10 mmol) in methanol (20 cm^3) to precipitate immediately dark red crystals. These were collected by suction filtration and washed with a small amount of methanol. The complex was recrystallized from methanol–*N*,*N*-dimethylformamide (dmf). Yield *ca.* 50% (Found: C, 35.0; H, 4.05; N, 14.7. Calc. for $C_{11}H_{15}ClCuN_4O_5$: C, 34.55; H, 3.95; N, 14.65%). M.p. 206 °C (decomp.); Λ_M 94.2 S cm^2 mol^{-1} (methanol); i.r. (Nujol), ν(NH) 3 350 cm^{-1}; $\lambda_{max.}$/nm ($\varepsilon_{max.}$/dm^3 mol^{-1} cm^{-1}) (methanol), 307 (8 700), 415 (sh) (140), 575 (160).

$[Ni(HL^1)][ClO_4]$. The nickel(II) complex was prepared similarly except that nickel(II) acetate tetrahydrate and sodium perchlorate were used. Yield *ca.* 60% (Found: C, 35.0; H, 4.05; N, 14.7. Calc. for $C_{11}H_{15}ClN_4NiO_5$: C, 35.0; H, 4.05; N, 14.7%). M.p. 260 °C (decomp.); Λ_M 99.0 S cm^2 mol^{-1} (methanol); i.r. (Nujol), ν(NH) 3 200 cm^{-1}; $\lambda_{max.}$/nm ($\varepsilon_{max.}$/dm^3 mol^{-1} cm^{-1}) (methanol), 334 (7 000), 502 (sh) (150); ^1H n.m.r. (CD_3CN), δ 10.96 (br, 1 H, NH), 7.89 (s, 1 H, –HC=N), 7.61 (d, 2 H, aromatic), 5.23 (s, 1 H, γ-H), 3.68—3.57 (m, 4 H, CH_2), 2.07 (s, 3 H, CH_3), 1.93 (s, 3 H, CH_3).

$[Cu(L^1)]$ (*deprotonated a-site component complex*). Complex (**1**) (3.84 g, 10 mmol) was suspended in chloroform (300 cm^3). To the suspension was slowly added NaH (600 mg, *ca.* 60% in oil) under stirring at room temperature. During the addition of NaH, complex (**1**) is gradually dissolved. After the evolution of hydrogen gas, the solution was further stirred for 1 h and then filtered. The red filtrate was evaporated to dryness under reduced pressure at ambient temperature. The resultant green crystals were suspended in diethyl ether (20 cm^3), filtered on a glass filter under reduced pressure, and washed with a small amount of diethyl ether. Attempts at recrystallization were unsuccessful, where the colour changes from green to black-green. Yield *ca.* 2 g; m.p. 161 °C; Λ_M 0.1 S cm^2 mol^{-1} (chloroform), i.r. (Nujol), disappearance of ν(NH) and ν(Cl–O); $\lambda_{max.}$/nm ($\varepsilon_{max.}$/dm^3 mol^{-1} cm^{-1}) (chloroform), 400 (395), 540 (150); solid state, 630 nm.

$[Cu(HL^2)][ClO_4]$ (**2**). Complex (**2**) was prepared similarly to (**1**) except that propane-1,3-diamine was used instead of ethylenediamine. Yield *ca.* 30% (Found: C, 36.2; H, 4.25; N, 14.15. Calc. for $C_{12}H_{17}ClCuN_4O_5$: C, 36.35; H, 4.30; N, 14.15%). M.p. 260 °C (decomp.); Λ_M 95.5 S cm^2 mol^{-1} (methanol); i.r. (Nujol), ν(NH) 3 250 cm^{-1}; $\lambda_{max.}$/nm ($\varepsilon_{max.}$/dm^3 mol^{-1} cm^{-1}) (methanol), 316 (8 500), 425 (150), 584 (70).

Synthesis of b-Site Component Complexes and Reference Complexes.—$[Cu(tfacac)_2]$ (*b-site component complex*). The complex was prepared by the method of Belford *et al.*[9]

Tris[2-(*N-ethylbenzimidazolyl*)*methyl*]*amine.* Tris(*N*-benzimidazolylmethyl)amine was prepared by the method of Thompson *et al.*[10] The N-ethylation was performed by the action of bromoethane in the presence of sodium hydroxide in tetrahydrofuran (thf) according to the method of McKee *et al.*[11]

$[Cu(tebima)][ClO_4]_2 \cdot 2H_2O$ (*b-site component complex*). To a solution of tebima (1 mmol) in methanol (20 cm^3) was added a solution of copper(II) perchlorate hexahydrate (1 mmol) in

methanol (10 cm^3). The solution was warmed on a water-bath for 30 min and allowed to stand overnight at room temperature. The precipitated yellow-green crystals were collected by suction filtration, washed with methanol, and dried.

$[Cu(tebima)(mim)][ClO_4]_2$ (*reference complex*). To a solution of $[Cu(tebima)][ClO_4]_2 \cdot 2H_2O$ (1 mmol) in 30 cm^3 of acetone was added *N*-methylimidazole (mim, 1.5 mmol). The solution was warmed on a water-bath for 10 min and allowed to stand overnight at room temperature. The precipitated blue-green crystals were collected by suction filtration, washed with methanol, and dried.

The b-site component and reference complexes as well as the ligands were identified by their elemental analyses (C, H, and N) and melting points. All compounds gave satisfactory elemental analytical results.

Synthesis of Imidazolate-bridged Binuclear Copper(II) Complexes.—Method A: $[Cu(L^1)Cu(tfacac)_2]$ (**3**). A mixture of complex (**1**) (382 mg, 1 mmol) and $[Cu(tfacac)_2]$ (369 mg, 1 mmol) in chloroform (150 cm^3) was refluxed for 10 min. To the suspension was slowly added a solution of triethylamine (100 mg, 1 mmol) in chloroform (10 cm^3). During the addition of triethylamine, complex (**1**) was gradually dissolved. After this was completed, the mixture was further refluxed for 30 min and then filtered. The filtrate was evaporated to dryness under reduced pressure and the residue was dissolved in diethyl ether (50 cm^3); the ether solution was again filtered. The filtrate was kept several days in air. During that time, reddish rhombic crystals, along with those of the b-site component complex $[Cu(tfacac)_2]$ precipitated. They were collected on a glass filter by suction filtration, washed thoroughly with diethyl ether until the washings no longer showed the blue colouration of $[Cu(tfacac)_2]$ (Found: C, 38.35; H, 3.95; N, 8.55. Calc. for $C_{21}H_{22}Cu_2F_6N_4O_5$: C, 38.7; H, 3.95; N, 8.60%. M.p. 167—170 °C, Λ_M 0.1 S cm^2 mol^{-1} (chloroform).

$[Cu(L^1)Cu(tebima)][ClO_4]_2 \cdot H_2O$. To a solution of complex (**1**) (382 mg, 1 mmol) in acetone (50 cm^3) was added a solution of triethylamine (100 mg, 1 mmol) in acetone (20 cm^3). The mixture was warmed on a water-bath for 30 min and then filtered. The filtrate was added to a solution of $[Cu(tebima)][ClO_4]_2 \cdot 2H_2O$ (790 mg, 1 mmol) in methanol (20 cm^3). The mixture was warmed on a water-bath for 1 h and then filtered. The filtrate was allowed to stand several days in a refrigerator; during that time, green microcrystals precipitated. These were collected by suction filtration, washed with methanol, and dried. Attempts to obtain crystals suitable for *X*-ray diffraction analysis were unsuccessful (Found: C, 46.95; H, 5.00; N, 14.5. Calc. for $C_{41}H_{47}Cl_2Cu_2N_{11}O_9 \cdot H_2O$: C, 46.75; H, 4.70; N, 14.6%). M.p. 259—260 °C; Λ_M 160 S cm^2 mol^{-1} (methanol); i.r. ν(Cl–O) 1 100 cm^{-1}. Thermogravimetric analysis (t.g.a.), mass loss 1.8 wt.%, calc. for H_2O, 1.7 wt.%.

$[Cu(L^1)Cu(tebima)][PF_6][ClO_4] \cdot Me_2CO$ (**4**). Single crystals suitable for *X*-ray diffraction analysis were obtained as follows. The a- and b-site component complexes were converted to the hexafluorophosphate salts by mixing each of the perchlorate salts with potassium hexafluorophosphate (1.5 times by mole ratio) in methanol. However, it was found that the precipitated compounds were the mixtures of the perchlorate and hexafluorophosphate salts. These compounds were used for the synthesis of imidazolate-bridged binuclear complex similarly to that for $[Cu(L^1)Cu(tebima)][ClO_4]_2 \cdot H_2O$ and thus single crystals suitable for *X*-ray work were obtained. The complex exhibits a dichromism (red/green) (Found: C, 46.0; H, 5.00; N, 13.4. Calc. for $C_{41}H_{47}ClCu_2F_6N_{11}O_5P \cdot C_3H_6O$: C, 46.4; H, 4.70; N, 13.5%). M.p. 251—253 °C; Λ_M 300 S cm^2 mol^{-1} (acetone); i.r. ν(Cl–O) 1 100 cm^{-1}; $\nu(PF_6^-)$ 840, 555 cm^{-1}. T.g.a., mass loss 5.1 wt.%; calc. for Me_2CO, 5.1 wt%.

Method B. Initially we prepared the imidazolate-bridged binuclear complexes by method A; single crystals of complexes (**3**) and (**4**) used for *X*-ray crystallography were obtained by this method. During the course of the study, the deprotonated a-site component complex $[Cu(L^1)]$ could be isolated. The imidazolate-bridged binuclear complexes can be synthesized by mixing the deprotonated complex and the b-site component complex in 1:1 mole ratio (method B). Method B is generally much more effective for the synthesis of the complexes.

Physical Measurements.—Elemental analyses were performed by Mr. Shinichi Miyazaki at the Technical Service Center of Kumamoto University. Melting points were measured on a Yanagimoto micromelting points apparatus and are uncorrected. Thermogravimetric analyses were carried out on a Shimadzu TGC 20 type microthermobalance at a heating rate of 5 °C min^{-1}, using *ca.* 5 mg samples for each run. Electrical conductivity measurements were carried out on a Denki Kagaku Keiki AOC-10 digital conductometer in 10^{-3} mol dm^{-3} solutions. Infrared spectra were measured on a JASCO A-702 spectrophotometer. Electronic spectra were obtained on a Hitachi UV 323 spectrophotometer. Magnetic susceptibilities were obtained by the Faraday method at liquid-nitrogen to room temperature, by the procedure reported previously.[12] The susceptibilities were corrected for the diamagnetism of the component atoms using Pascal's constants. Electron spin resonance spectra at *X*-band frequencies were obtained with a JEOL JES-FE3X spectrometer at liquid-nitrogen and at room temperatures. ^1H N.m.r. spectra were obtained on a JEOL JNM-GX instrument at 400 MHz.

X-Ray Diffraction Analyses.—Diffraction data were obtained on a Rigaku Denki AFC-5R four-circle diffractometer at the Institute for Molecular Science, Okazaki National Institute, for complex (**1**) and on a Rigaku Denki AFC-5 four-circle diffractometer at the Faculty of Science, Kyushu University, for complexes (**2**)—(**4**), using graphite-monochromatized Mo-K_α radiation at ambient temperature (20 ± 1 °C). Pertinent crystallographic parameters are summarized in Table 1. Three standard reflections were monitored every 100 measurements and their intensities showed no decay. Reflection data were corrected for Lorentz-polarization effects but not for absorption.

The structures were solved by the standard heavy-atom method and refined by block-diagonal least-squares calculations. Reliability factors are defined as $R = \Sigma||F_o| - |F_c||/\Sigma|F_o|$ and $R' = [\Sigma w(|F_o| - |F_c|)^2/\Sigma w|F_o|^2]^{\frac{1}{2}}$, where the weights were taken as $w = 1$.

$[Cu(HL^1)][ClO_4]$ (**1**). The copper atom was obtained by explanation of the Harker peaks of a three-dimensional Patterson synthesis, and successive Fourier syntheses on the basis of the copper atom revealed all the non-hydrogen atoms. Hydrogen atoms were located by difference Fourier synthesis. The non-hydrogen and hydrogen atoms were refined anisotropically and isotropically, respectively. A final difference Fourier synthesis showed no significant features (all <0.3 e $Å^{-3}$).

$[Cu(HL^2)][ClO_4]$ (**2**). The copper atom was obtained by a three-dimensional Patterson synthesis and successive Fourier and difference Fourier syntheses showed the non-hydrogen and hydrogen atoms. The non-hydrogen and hydrogen atoms were refined anisotropically and isotropically, respectively. A final difference Fourier synthesis was featureless (all <0.4 e $Å^{-3}$).

$[Cu(L^1)Cu(tfacac)_2]$ (**3**). The two copper atoms were obtained by three-dimensional Patterson synthesis, and successive Fourier syntheses on the basis of the two copper atoms revealed all non-hydrogen atoms. The non-hydrogen atoms were refined anisotropically and successive difference Fourier syntheses located all hydrogen atoms. In the final least-squares calculation, hydrogen atoms were refined isotropically. The final

Table 1. Summary of crystal data, intensity collection, and structure refinement*

	(1)	(2)	(3)	(4)
Complex	$[Cu(HL^1)][ClO_4]$	$[Cu(HL^2)][ClO_4]$	$[Cu(L^1)Cu(tfacac)_2]$	$[Cu(L^1)Cu(tebima)][PF_6][ClO_4]\cdot Me_2CO$
Formula	$C_{11}H_{15}ClCuN_4O_5$	$C_{12}H_{17}ClCuN_4O_5$	$C_{21}H_{22}Cu_2F_6N_4O_5$	$C_{44}H_{53}ClCu_2F_6N_{11}O_6P$
M	382.26	396.25	651.50	1 139.5
Crystal system	monoclinic	triclinic	triclinic	triclinic
Space group	$P2_1/n$	$P\bar{1}$	$P\bar{1}$	$P\bar{1}$
a/Å	22.146(2)	10.551(4)	11.462(4)	13.131(5)
b/Å	9.659(1)	11.602(3)	16.708(8)	19.285(6)
c/Å	7.126(1)	7.307(1)	7.692(2)	10.878(4)
α/°	90.00	98.95(1)	93.96(3)	93.89(2)
β/°	98.35(1)	96.99(2)	109.98(2)	92.83(2)
γ/°	90.00	113.04(2)	71.74(3)	114.64(2)
U/Å^3	1 508.2	796.5	1 313.6	2 488.8
Z	4	2	2	2
D_c/g cm^{-3}	1.683	1.652	1.647	1.520
D_m/g cm^{-3}	1.68	1.63	1.61	1.52
Crystal size	0.2 × 0.2 × 0.3	0.2 × 0.2 × 0.2	0.2 × 0.2 × 0.2	0.5 × 0.4 × 0.3
μ(Mo-K_α)/cm^{-1}	16.9	16.0	17.4	10.5
F(000)	780	406	656	1 172
2θ range (°)	2—50	2.5—50	2.5—50	2.5—48
Octant measured	$+h, +k, \pm l$	$+h, \pm k, \pm l$	$+h, \pm k, \pm l$	$+h, \pm k, \pm l$
No. of unique data	2 075	2 363	4 017	4 767
R	3.8	4.8	4.3	8.9
R'	5.7	5.6	4.3	9.6

* Data common to all structures: Rigaku AFC-5 diffractometer [AFC-5R for (**1**)]; θ—2θ scan, scan width (1.2 + 0.5 tanθ)°, scan speed 8° min^{-1}.

Table 2. Fractional atomic co-ordinates (× 10^4) for $[Cu(HL^1)][ClO_4]$ (**1**)

Atom	X/a	Y/b	Z/c	Atom	X/a	Y/b	Z/c
Cu	219(1)	568(1)	2 297(1)	C(6)	968(3)	2 958(6)	2 295(9)
O(1)	453(1)	−1 226(3)	1 665(5)	C(7)	431(3)	3 487(6)	3 127(11)
N(1)	979(2)	1 474(4)	2 062(5)	C(8)	−552(2)	2 544(5)	3 497(7)
N(2)	−29(2)	2 413(4)	3 034(6)	C(9)	−908(2)	1 300(5)	3 397(6)
N(3)	−615(2)	111(3)	2 694(5)	C(10)	−1 492(2)	969(6)	3 612(7)
N(4)	−1 557(2)	−389(4)	3 234(5)	C(11)	−1 025(2)	−888(5)	2 810(6)
C(1)	1 123(3)	−3 048(6)	1 332(8)	Cl	3 209(1)	−451(1)	7 691(2)
C(2)	1 013(2)	−1 543(5)	1 530(6)	O(2)	3 808(2)	−656(4)	7 243(6)
C(3)	1 491(2)	−629(5)	1 588(7)	O(3)	2 843(2)	174(6)	6 168(8)
C(4)	1 481(2)	804(6)	1 830(6)	O(4)	2 943(2)	−1 719(4)	8 153(6)
C(5)	2 068(2)	1 615(8)	1 826(8)	O(5)	3 253(3)	428(5)	9 260(8)

Table 3. Fractional atomic co-ordinates (× 10^4) for $[Cu(HL^2)][ClO_4]$ (**2**)

Atom	X/a	Y/b	Z/c	Atom	X/a	Y/b	Z/c
Cu	665(1)	396(1)	2 901(1)	C(7)	3 986(6)	1 361(8)	3 733(12)
O(1)	−818(4)	709(4)	3 785(6)	C(8)	3 413(7)	450(8)	1 806(12)
N(1)	2 076(5)	2 146(5)	3 870(7)	C(9)	1 302(7)	−1 470(7)	798(9)
N(2)	1 890(5)	−313(5)	1 645(7)	C(10)	−173(7)	−2 131(6)	771(8)
N(3)	−743(5)	−1 371(5)	1 664(7)	C(11)	−1 159(8)	−3 343(7)	117(9)
N(4)	−2 362(6)	−3 327(5)	596(8)	C(12)	−2 073(7)	−2 145(6)	1 514(9)
C(1)	−2 212(8)	1 845(8)	4 338(12)	Cl	6 138(2)	3 184(1)	−731(2)
C(2)	−805(6)	1 818(6)	4 183(8)	O(2)	5 501(5)	4 044(5)	−735(10)
C(3)	355(7)	2 943(6)	4 476(10)	O(3)	5 187(6)	1 919(5)	−1 531(11)
C(4)	1 747(7)	3 097(6)	4 392(9)	O(4)	7 155(8)	3 529(7)	−1 808(12)
C(5)	2 853(9)	4 469(7)	4 961(12)	O(5)	6 722(12)	3 227(10)	1 043(10)
C(6)	3 610(6)	2 485(7)	3 918(11)				

difference Fourier synthesis showed no significant features (all <0.3 e Å^{-3}).

$[Cu(L^1)Cu(tebima)][PF_6][ClO_4]\cdot Me_2CO$ (**4**). The two copper atoms were obtained by three-dimensional Patterson synthesis. Successive Fourier and difference Fourier syntheses revealed non-hydrogen atoms, where the oxygen atoms of the perchlorate anion were subject to disorder. In the final least-squares calculation, non-hydrogen atoms of the cation $[Cu(L^1)Cu(tebima)]^{2+}$, the P and Cl atoms of the anions were refined anisotropically, and the other non-hydrogen atoms of the anions and the solvent (acetone) were refined isotropically. The positions of the hydrogen atoms were calculated, but not refined, and included in the structure factor calculations. The final difference Fourier synthesis showed several peaks around the counter anions (*ca.* 1.0 e Å^{-3}).

The calculations were carried out on the HITAC M 200H

Table 4. Fractional atomic co-ordinates ($\times 10^4$) for $[Cu(L^1)Cu(tfacac)_2]$ (**3**)

Atom	*X/a*	*Y/b*	*Z/c*	Atom	*X/a*	*Y/b*	*Z/c*
Cu(1)	9 071(1)	−224(0)	1 288(1)	O(3)	11 103(3)	2 917(2)	6 086(4)
O(1)	7 289(3)	306(2)	24(5)	O(4)	8 566(3)	3 569(2)	2 236(4)
N(1)	9 179(4)	−1 297(2)	200(5)	O(5)	7 490(3)	3 070(2)	4 780(4)
N(2)	10 942(4)	−724(2)	2 483(5)	F(1)	13 565(3)	3 817(2)	7 896(6)
N(3)	9 411(3)	727(2)	2 832(5)	F(2)	13 451(3)	2 809(3)	6 107(5)
N(4)	9 704(3)	1 855(2)	4 432(5)	F(3)	13 582(3)	2 650(3)	8 851(6)
C(1)	5 181(6)	501(4)	−2 111(11)	F(4)	5 118(5)	3 719(5)	5 131(7)
C(2)	6 542(5)	−62(3)	−1 201(8)	F(5)	4 177(3)	3 670(3)	2 336(6)
C(3)	6 937(5)	−884(3)	−1 656(8)	F(6)	5 313(5)	2 583(4)	3 870(10)
C(4)	8 174(5)	−1 487(3)	−953(7)	C(12)	8 993(5)	5 445(3)	7 417(7)
C(5)	8 292(6)	−2 368(3)	−1 629(9)	C(13)	9 592(4)	4 581(3)	6 870(6)
C(6)	10 453(5)	−1 943(3)	926(7)	C(14)	10 941(4)	4 279(3)	7 240(6)
C(7)	11 524(5)	−1 553(3)	1 884(7)	C(15)	11 572(4)	3 496(3)	6 861(6)
C(8)	11 526(4)	−281(3)	3 676(6)	C(16)	13 052(5)	3 201(3)	7 427(7)
C(9)	10 712(4)	542(2)	3 909(6)	C(17)	7 032(7)	4 179(4)	−733(7)
C(10)	10 871(4)	1 242(3)	4 882(6)	C(18)	7 405(4)	3 795(3)	1 241(6)
C(11)	8 856(4)	1 508(3)	3 198(6)	C(19)	6 370(4)	3 731(3)	1 763(7)
Cu(2)	9 260(0)	3 045(0)	5 091(1)	C(20)	6 486(4)	3 400(3)	3 406(6)
O(2)	8 831(3)	4 160(2)	6 108(4)	C(21)	5 265(5)	3 373(4)	3 720(8)

Table 5. Fractional atomic co-ordinates ($\times 10^4$) for $[Cu(L^1)Cu(tebima)][PF_6][ClO_4]\cdot Me_2CO$ (**4**)

Atom	*X/a*	*Y/b*	*Z/c*	Atom	*X/a*	*Y/b*	*Z/c*
Cu(1)	1 291(1)	1 341(1)	1 294(1)	C(16)	2 097(10)	−346(7)	5 229(10)
O	2 334(7)	1 093(5)	491(7)	C(17)	2 592(11)	−801(7)	5 676(11)
N(1)	164(8)	1 035(6)	−61(9)	C(18)	3 709(10)	−489(7)	6 178(10)
N(2)	191(7)	1 537(6)	2 223(9)	C(19)	4 285(9)	295(6)	6 174(9)
N(3)	2 195(7)	1 756(6)	2 882(8)	C(20)	6 175(10)	550(7)	7 218(11)
N(4)	3 301(7)	2 246(5)	4 624(8)	C(21)	5 977(12)	431(9)	8 558(13)
C(1)	3 238(12)	813(9)	−1 136(12)	C(22)	7 112(9)	3 261(8)	5 458(12)
C(2)	2 220(11)	866(7)	−664(11)	C(23)	6 598(10)	3 721(7)	4 888(11)
C(3)	1 272(12)	702(8)	−1 466(12)	C(24)	5 286(9)	4 030(6)	4 212(9)
C(4)	303(11)	779(7)	−1 143(11)	C(25)	4 294(9)	4 105(7)	3 928(10)
C(5)	−643(13)	549(9)	−2 198(13)	C(26)	4 351(11)	4 712(7)	3 302(10)
C(6)	−827(10)	1 183(8)	190(13)	C(27)	5 396(12)	5 253(7)	2 958(11)
C(7)	−911(10)	1 293(9)	1 541(14)	C(28)	6 363(11)	5 193(7)	3 253(11)
C(8)	473(9)	1 816(7)	3 325(11)	C(29)	6 303(10)	4 581(7)	3 869(10)
C(9)	1 615(9)	1 968(7)	3 757(10)	C(30)	8 348(11)	4 805(9)	4 255(14)
C(10)	2 289(9)	2 255(7)	4 826(10)	C(31)	8 716(15)	4 595(14)	3 143(22)
C(11)	3 206(9)	1 949(7)	3 455(10)	C(32)	6 658(9)	3 480(7)	7 529(10)
Cu(2)	4 699(1)	2 564(1)	5 684(1)	C(33)	5 621(9)	3 310(6)	8 170(10)
N(5)	6 394(7)	2 889(5)	6 451(8)	C(34)	3 861(10)	2 943(6)	8 502(10)
N(6)	4 594(7)	1 519(5)	5 895(8)	C(35)	2 707(10)	2 653(7)	8 422(11)
N(7)	5 371(7)	792(5)	6 622(8)	C(36)	2 233(11)	2 792(8)	9 467(13)
N(8)	5 488(7)	3 493(5)	4 849(8)	C(37)	2 905(13)	3 180(8)	10 562(12)
N(9)	7 120(7)	4 362(6)	4 337(9)	C(38)	4 036(12)	3 454(7)	10 650(11)
N(10)	4 589(7)	2 919(5)	7 602(7)	C(39)	4 516(11)	3 347(7)	9 606(10)
N(11)	5 622(8)	3 571(5)	9 350(8)	C(40)	6 593(11)	4 098(8)	10 165(11)
C(12)	6 531(10)	2 192(7)	6 834(12)	C(41)	6 750(12)	4 906(8)	10 052(12)
C(13)	5 500(9)	1 500(6)	6 439(9)	Cl	−138(3)	2 897(3)	6 738(4)
C(14)	3 797(9)	750(6)	5 720(9)	P	6 470(4)	2 222(2)	11 747(4)
C(15)	2 669(9)	427(7)	5 225(10)				
O(1)[a,b]	−90(2)	255(1)	568(2)	F(2)[a]	739(1)	236(1)	1 273(1)
O(2)[a,b]	88(2)	351(1)	749(2)	F(3)[a]	660(1)	149(1)	1 134(1)
O(3)[a,c]	−36(3)	349(2)	611(3)	F(4)[a]	583(2)	216(1)	1 054(2)
O(4)[a,c]	−27(4)	251(2)	794(4)	F(5)[a]	564(2)	179(1)	1 264(2)
O(5)[a,b]	32(2)	231(1)	654(2)	F(6)[a]	733(2)	268(1)	1 091(2)
O(6)[a,b]	−64(2)	341(1)	722(2)	O(S)[a]	146(2)	479(1)	236(2)
O(7)[a,c]	92(2)	323(2)	617(2)	C(S1)[a]	73(2)	416(2)	177(2)
O(8)[a,c]	−91(2)	243(2)	758(3)	C(S2)[a]	60(2)	354(2)	256(3)
F(1)[a]	627(1)	291(1)	1 221(1)	C(S3)[a]	18(3)	401(2)	67(3)

[a] Atomic co-ordinates are multiplied by 10^3. [b] Occupancy factor 0.6. [c] Occupancy factor 0.4.

computer at the Computer Center of the Institute for Molecular Science, Okazaki National Institute for complex (**1**) and on the FACOM M 386 computer at the Computer Center of Kyushu University for complexes (**2**)—(**4**) with the Universal Crystallographic Computation Program System UNICS III.[13] Atomic scattering factors for non-hydrogen atoms were taken from ref.

Table 6. Bond distances (Å) and angles (°) for the cation of $[Cu(HL^1)][ClO_4]$ (**1**)

Cu–O(1)	1.881(3)	N(1)–C(6)	1.443(7)	C(1)–C(2)	1.483(7)	C(9)–C(10)	1.361(6)
Cu–N(1)	1.925(3)	C(6)–C(7)	1.494(9)	C(2)–C(3)	1.375(6)	C(11)–N(4)	1.342(6)
Cu–N(2)	1.959(3)	C(7)–N(2)	1.448(7)	C(3)–C(4)	1.395(7)	N(4)–C(11)	1.347(6)
Cu–N(3)	2.004(3)	N(2)–C(8)	1.256(6)	C(4)–C(5)	1.518(7)	C(11)–N(3)	1.320(5)
O(1)–C(2)	1.293(5)	C(8)–C(9)	1.433(6)	C(4)–N(1)	1.317(6)	N(3)–C(9)	1.391(5)
O(1)–Cu–N(1)	97.1(1)	N(1)–C(6)–C(7)	114.3(5)	C(2)–C(3)–C(4)	127.8(4)	C(8)–C(9)–C(10)	135.6(4)
N(1)–Cu–N(2)	83.7(1)	N(2)–C(7)–C(6)	109.4(4)	N(1)–C(4)–C(3)	122.1(4)	N(4)–C(10)–C(9)	106.4(4)
N(2)–Cu–N(3)	80.8(1)	Cu–N(2)–C(7)	116.1(3)	N(1)–C(4)–C(5)	119.0(5)	Cu–N(3)–C(9)	110.6(2)
N(3)–Cu–O(1)	98.2(1)	Cu–N(2)–C(8)	117.8(3)	C(3)–C(4)–C(5)	118.7(4)	Cu–N(3)–C(11)	143.1(3)
Cu–O(1)–C(2)	122.4(3)	C(7)–N(2)–C(8)	125.8(4)	Cu–N(1)–C(4)	123.4(3)	C(9)–N(3)–C(11)	105.7(3)
O(1)–C(2)–C(1)	114.3(4)	N(2)–C(8)–C(9)	115.1(4)	Cu–N(1)–C(6)	114.3(3)	C(10)–N(4)–C(11)	108.8(3)
O(1)–C(2)–C(3)	125.9(4)	N(3)–C(9)–C(8)	115.5(3)	C(4)–N(1)–C(6)	122.0(4)	N(3)–C(11)–N(4)	110.2(4)
C(1)–C(2)–C(3)	119.7(4)	N(3)–C(9)–C(10)	108.7(4)				

Table 7. Bond distances (Å) and angles (°) for the cation of $[Cu(HL^2)][ClO_4]$ (**2**)

Cu–O(1)	1.901(5)	C(6)–C(7)	1.493(13)	C(2)–C(3)	1.356(8)	C(10)–C(11)	1.344(8)
Cu–N(1)	1.940(4)	C(7)–C(8)	1.516(11)	C(3)–C(4)	1.418(11)	C(11)–N(4)	1.360(12)
Cu–N(2)	2.018(6)	C(8)–N(2)	1.483(8)	C(4)–C(5)	1.508(8)	N(4)–C(12)	1.328(9)
Cu–N(3)	1.985(4)	N(2)–C(9)	1.249(8)	C(4)–N(1)	1.297(10)	C(12)–N(3)	1.319(7)
O(1)–C(1)	1.267(9)	C(9)–C(10)	1.440(9)	N(1)–C(6)	1.502(8)	N(3)–C(10)	1.376(10)
C(1)–C(2)	1.510(12)						
O(1)–Cu–N(1)	95.1(2)	C(6)–C(7)–C(8)	114.1(7)	C(2)–C(3)–C(4)	126.8(7)	N(3)–C(10)–C(11)	110.4(6)
N(1)–Cu–N(2)	97.4(2)	C(7)–C(8)–N(2)	108.2(6)	C(3)–C(4)–N(1)	123.6(5)	C(10)–C(11)–N(4)	105.0(7)
N(2)–Cu–N(3)	79.5(2)	C(8)–N(2)–Cu	122.6(4)	C(3)–C(4)–C(5)	114.5(7)	C(11)–N(4)–C(12)	108.8(5)
N(3)–Cu–O(1)	87.7(2)	C(8)–N(2)–C(9)	121.0(7)	C(5)–C(4)–N(1)	121.8(7)	N(4)–C(12)–N(3)	110.7(7)
Cu–O(1)–C(2)	123.3(4)	Cu–N(2)–C(9)	116.2(5)	C(4)–N(1)–Cu	122.1(4)	C(12)–N(3)–C(10)	104.9(5)
O(1)–C(2)–C(1)	115.5(5)	N(2)–C(9)–C(10)	116.4(7)	C(4)–N(1)–C(6)	116.4(5)	C(12)–N(3)–Cu	141.0(5)
O(1)–C(2)–C(3)	125.1(7)	C(9)–C(10)–N(3)	113.9(5)	Cu–N(1)–C(6)	121.1(4)	Cu–N(3)–C(10)	113.6(3)
C(1)–C(2)–C(3)	119.3(7)	C(9)–C(10)–C(11)	135.5(8)	N(1)–C(6)–C(7)	114.9(5)		

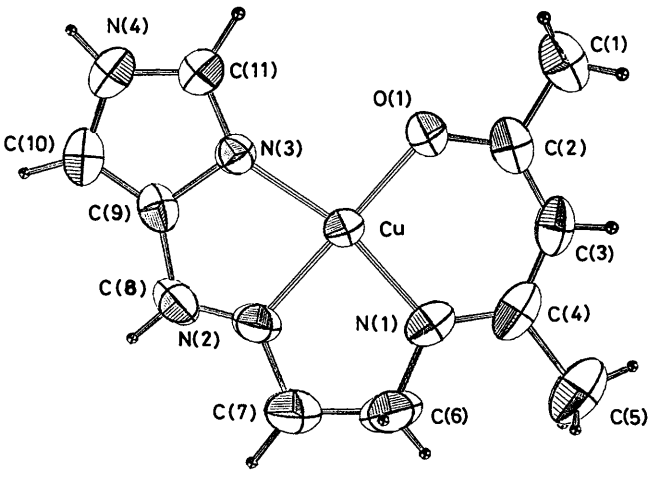

Figure 1. Perspective view of $[Cu(HL^1)]^+$ with the atom numbering scheme

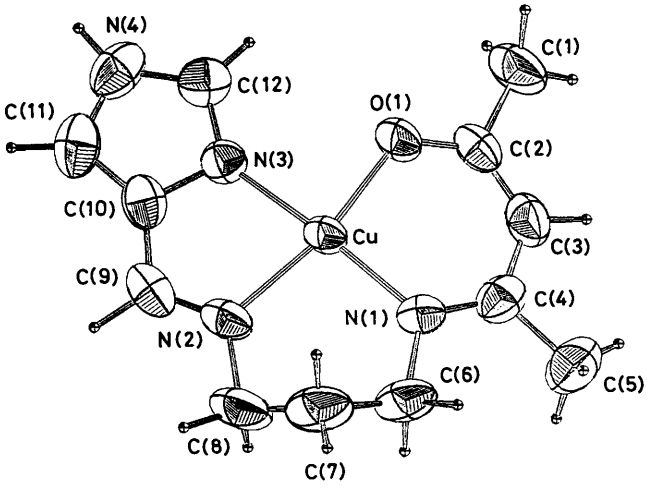

Figure 2. Perspective view of $[Cu(HL^2)]^+$ with the atom numbering scheme

14 and those for hydrogen from Stewart *et al.*[15] Corrections for the effects of anomalous dispersion for the non-hydrogen atoms were made in the structure factor calculations. Positional parameters of non-hydrogen atoms for complexes (**1**)—(**4**) are given in Tables 2—5 respectively. Additional material available from the Cambridge Crystallographic Data Centre comprises H-atom co-ordinates and thermal parameters.

Results and Discussion

Mononuclear Copper(II) *Complexes* (**1**) *and* (**2**) *with Unsymmetrical Quadridentate Ligands involving an Imidazole Moiety.*—Several unsymmetrical quadridentate Schiff-base ligands composed of β-diketone, diamine, and salicylaldehyde derivatives have been reported so far.[16] These ligands have been prepared by mixing β-diketone, diamine, and salicylaldehyde

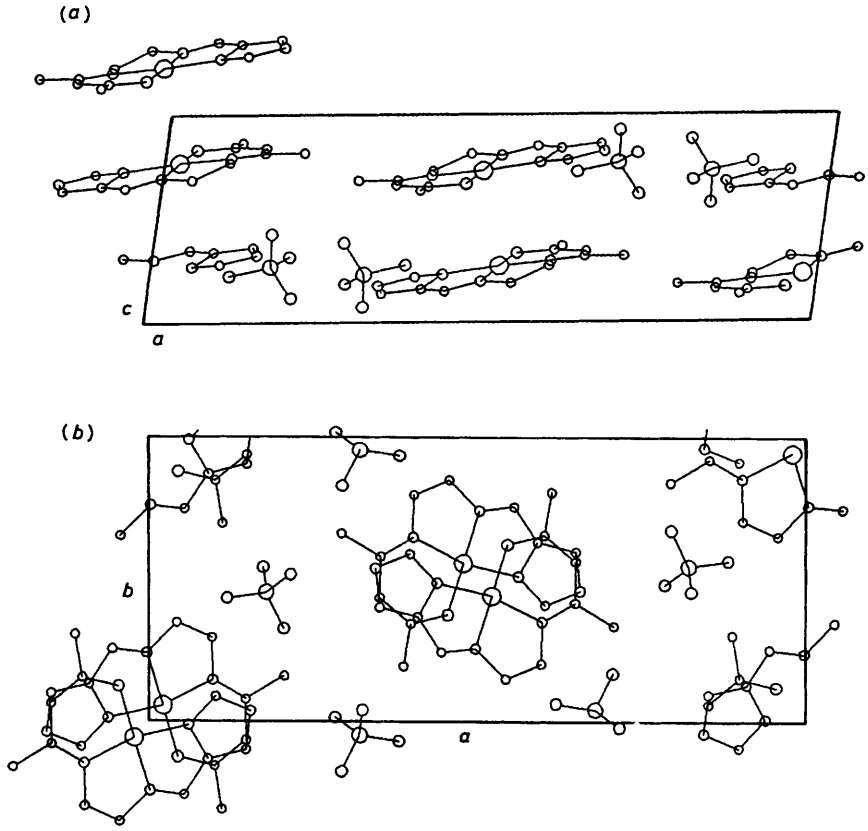

Figure 3. Crystal structure of $[Cu(HL^1)][ClO_4]$ (**1**) projected along (*a*) the *b* axis and (*b*) the *c* axis

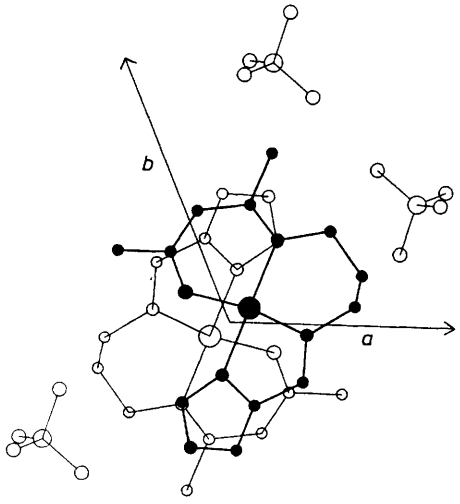

Figure 4. Crystal structure of $[Cu(HL^2)][ClO_4]$ (**2**) projected along the *c* axis

derivatives initially, then, after the reaction with metal ion, separating the unsymmetrical ligand from the symmetrical ligands as sub-products by column chromatography. Complexes (**1**) and (**2**) have been prepared by a stepwise reaction procedure. The 1:1 condensation products of acetylacetone and ethylenediamine or propane-1,3-diamine were prepared under highly dilute conditions according to the method of Costes *et al.*[8] Then one equivalent of 4-formylimidazole was reacted with the 1:1 condensation product to produce the unsymmetrical quadridentate ligand composed of acetylacetone, ethylenediamine or propane-1,3-diamine, and 4-formylimidazole (1:1:1). Reaction of the ligands with copper(II) perchlorate hexahydrate gave complexes (**1**) and (**2**).

The molar electrical conductivities in methanol of (**1**) and (**2**) are 94.2 and 95.5 S cm^2 mol^{-1}, respectively, which are in the range expected for 1:1 electrolytes (80—115 S cm^2 mol^{-1}).[17] This implies that the ligands co-ordinate to copper(II) uninegative ions, with perchlorate as counter anion. Infrared spectra of (**1**) and (**2**) showed the characteristic bands assignable to ν(NH) (imidazole) at *ca.* 3 300 cm^{-1} and ν(Cl–O) (perchlorate) at *ca.* 1 100 cm^{-1}. Electronic spectra consist of a broad band in the visible region assignable to a *d–d* transition and several bands in the u.v. region assignable to charge-transfer transitions. The *d–d* band maxima for (**1**) and (**2**) vary depending on the solvent, $\lambda_{max.}$/nm: 550 (Me_2CO, MeCN), 566 (dmf), 575 (MeOH) for (**1**); 560 (MeCN), 580 (dmf), 584 (MeOH) for (**2**). In addition, the band maxima measured in methanol shift to shorter wavelengths on addition of triethylamine. The result indicates that the *d–d* band maxima depend on the deprotonation of the imidazole proton.

The ^1H n.m.r. spectrum of $[Ni(HL^1)][ClO_4]$ gives direct evidence of the formation of an unsymmetrical quadridentate ligand. As anticipated, the spectrum consists of two methyl and one methine signals of the acetylacetone moiety, methylene signals (multiplet) of the ethylenediamine moiety, and aromatic imine and imidazole proton signals of the 4-formylimidazole moiety; the integrated intensity ratio being 1:1:1, consistent with the structure of the ligand.

Deprotonated a-Site Component Complex $[Cu(L^1)]$.—The deprotonated complex $[Cu(L^1)]$ has been obtained as green crystals by the reaction of (**1**) and NaH in chloroform. The i.r.

Table 8. Relevant bond distances (Å) and angles (°) for the cation of $[Cu(L^1)Cu(tfacac)_2]$ (**3**)

a-Site							
Cu(1)–O(1)	1.878(3)	N(3)–N(11)	1.319(5)	N(1)–C(4)	1.307(6)	C(3)–C(4)	1.405(6)
Cu(1)–N(1)	1.911(3)	N(4)–C(10)	1.354(4)	N(1)–C(6)	1.465(5)	C(4)–C(5)	1.507(7)
Cu(1)–N(2)	1.944(3)	N(4)–C(11)	1.352(5)	N(2)–C(7)	1.455(5)	C(6)–C(7)	1.514(7)
Cu(1)–N(3)	1.974(3)	C(1)–C(2)	1.494(7)	N(2)–C(8)	1.279(5)	C(8)–C(9)	1.438(5)
O(1)–C(2)	1.303(6)	C(2)–C(3)	1.365(7)	N(3)–C(9)	1.381(5)	C(9)–C(10)	1.371(6)
b-Site							
Cu(2)–N(4)	1.966(3)	C(15)–C(16)	1.521(6)	O(3)–C(15)	1.268(5)	F(2)–C(16)	1.307(7)
Cu(2)–O(2)	1.953(3)	C(17)–C(18)	1.555(7)	O(4)–C(18)	1.236(4)	F(3)–C(16)	1.323(6)
Cu(2)–O(3)	1.930(3)	C(18)–C(19)	1.411(8)	O(5)–C(20)	1.264(4)	F(4)–C(21)	1.232(8)
Cu(2)–O(4)	2.203(3)	C(19)–C(20)	1.362(7)	C(12)–C(13)	1.491(6)	F(5)–C(21)	1.309(5)
Cu(2)–O(5)	1.947(3)	C(20)–C(21)	1.515(8)	C(13)–C(14)	1.399(6)	F(6)–C(21)	1.314(9)
O(2)–C(13)	1.256(5)	F(1)–C(16)	1.310(7)	C(14)–C(15)	1.348(5)		
a-Site							
O(1)–Cu(1)–N(1)	97.3(1)	C(10)–N(4)–C(11)	104.9(3)	Cu(1)–N(1)–C(6)	115.1(2)	N(1)–C(6)–C(7)	111.5(3)
O(1)–Cu(1)–N(2)	175.9(1)	O(1)–C(2)–C(1)	114.0(4)	C(4)–N(1)–C(6)	120.8(3)	N(2)–C(7)–C(6)	108.6(2)
O(1)–Cu(1)–N(3)	97.2(1)	O(1)–C(2)–C(3)	124.4(4)	Cu(1)–N(2)–C(7)	116.2(2)	N(2)–C(8)–C(9)	115.3(3)
N(1)–Cu(1)–N(2)	83.9(1)	C(1)–C(2)–C(3)	121.6(5)	Cu(1)–N(2)–C(8)	116.4(2)	N(3)–C(9)–C(8)	114.9(3)
N(1)–Cu(1)–N(3)	165.3(1)	C(2)–C(3)–C(4)	128.6(5)	C(7)–N(2)–C(8)	127.4(3)	N(3)–C(9)–C(10)	107.7(3)
N(2)–Cu(1)–N(3)	81.9(1)	N(1)–C(4)–C(3)	122.2(4)	Cu(1)–N(3)–C(9)	111.5(2)	C(8)–C(9)–C(10)	137.3(4)
Cu(1)–O(1)–C(2)	123.5(2)	N(1)–C(4)–C(5)	121.4(4)	Cu(1)–N(3)–C(11)	143.2(2)	N(4)–C(10)–C(9)	108.9(3)
Cu(1)–N(1)–C(4)	123.7(3)	C(3)–C(4)–C(5)	116.5(4)	C(9)–N(3)–C(11)	105.3(3)	N(3)–C(11)–N(4)	113.2(3)
b-Site							
C(10)–N(4)–Cu(2)	130.5(3)	O(3)–C(15)–C(16)	111.0(3)	O(4)–Cu(2)–O(5)	89.4(1)	F(1)–C(16)–C(15)	113.3(4)
C(11)–N(4)–Cu(2)	124.3(2)	C(14)–C(15)–C(16)	120.1(4)	Cu(2)–O(2)–C(13)	127.5(2)	F(2)–C(16)–F(3)	105.6(4)
N(4)–Cu(2)–O(2)	171.2(1)	O(4)–C(18)–C(17)	118.8(5)	Cu(2)–O(3)–C(15)	124.2(2)	F(2)–C(16)–C(15)	112.0(4)
N(4)–Cu(2)–O(3)	88.6(1)	O(4)–C(18)–C(19)	124.6(4)	Cu(2)–O(4)–C(18)	123.6(3)	F(3)–C(16)–C(15)	110.9(5)
N(4)–Cu(2)–O(4)	95.6(1)	C(17)–C(18)–C(19)	116.6(4)	Cu(2)–O(5)–C(20)	125.6(3)	F(4)–C(21)–F(5)	108.2(5)
N(4)–Cu(2)–O(5)	91.0(1)	C(19)–C(20)–C(21)	118.7(3)	O(2)–C(13)–C(12)	116.6(4)	F(4)–C(21)–F(6)	107.6(7)
O(2)–Cu(2)–O(3)	91.5(1)	O(5)–C(20)–C(19)	130.4(4)	O(2)–C(13)–C(14)	123.8(3)	F(4)–C(20)–C(21)	113.6(5)
O(2)–Cu(2)–O(4)	92.9(1)	O(5)–C(20)–C(21)	110.9(4)	C(12)–C(13)–C(14)	119.7(4)	F(5)–C(21)–F(6)	101.9(5)
O(2)–Cu(2)–O(5)	86.5(1)	F(1)–C(16)–F(2)	107.3(5)	C(13)–C(14)–C(15)	123.7(4)	F(5)–C(21)–C(20)	115.3(5)
O(3)–Cu(2)–O(4)	106.4(1)	F(1)–C(16)–F(3)	107.4(4)	O(3)–C(15)–C(14)	128.9(4)	F(6)–C(21)–C(20)	109.5(4)
O(3)–Cu(2)–O(5)	164.1(1)						

bands due to ν(N–H) (imidazole) and ν(Cl–O) (perchlorate) observed in the spectrum of the starting complex (**1**) disappear in that of $[Cu(L^1)]$. The molar electrical conductance measured in chloroform is zero, being consistent with the formulation. The complex $[Cu(L^1)]$ dissolves well in organic solvents such as methanol, acetone, acetonitrile, and chloroform, the colour changing from green in the solid to red in solution. In the solid state, the reflectance spectrum exhibits a *d–d* transition at 630 nm, while in chloroform the absorption spectrum exhibits a *d–d* transition at 540 nm, indicating different co-ordination geometries in the solid and in solution. It is considered that in solution the deprotonated species $[Cu(L^1)]$ exists independently, on the basis of the similarity of the electronic spectra of $[Cu(HL^1)][ClO_4]$ and $[Cu(L^1)]$. However, in the solid state the deprotonated complex has an imidazolate-bridged polynuclear structure in which each copper ion is five-co-ordinate with a neighbouring imidazolate nitrogen as axial ligand, on the basis of the crystal structure of the related copper(II) complex of the monoanionic 1:1:1 condensation product of salicylaldehyde, propane-1,3-diamine, and 4-formylimidazole.[18]

Structures of Complexes (**1**) *and* (**2**).—Perspective drawings of complexes (**1**) and (**2**) are shown in Figures 1—4, with the atom numbering schemes; bond distances and angles are given in Tables 6 and 7. The present *X*-ray analyses verified the structures of the copper(II) complexes with unsymmetrical quadridentate ligands composed of the condensation products of acetylacetone, ethylenediamine, or propane-1,3-diamine, and 4-formylimidazole in the mole ratio 1:1:1.

In both complexes (**1**) and (**2**), the copper(II) ion assumes a square-planar co-ordination geometry with the maximum deviation of the component atoms 0.05 Å from the mean plane defined by Cu, O(1), N(1), and N(3). The saturated five-membered chelate ring of (**1**) adopts a *gauche* conformation, where the atoms C(6) and C(7) deviate −0.15 Å and 0.05 Å from the plane of the Cu, N(1), and N(2) atoms. The saturated six-membered chelate ring of (**2**) adopts a boat conformation, where the atoms Cu and C(7) deviate 0.18 and 0.72 Å from the plane defined by N(1), N(2), C(6), and C(8).

Crystal packing diagrams of (**1**) and (**2**) are shown in Figures 3 and 4, respectively. A weak hydrogen bond between the imidazole nitrogen atom and the oxygen atom of the perchlorate anion through the imidazole proton is observed in both complexes. The distance is 2.95 Å [N(4)–O(3)] for (**1**) and 2.92 Å [N(4)–O(2)] for (**2**). The planar cation $[Cu(HL^1)]^+$ or $[Cu(HL^2)]^+$ and the symmetry related cation [$-x$, $-y$, $-z$ for (**1**); $-x$, $-y$, $-z+1$ for (**2**)] shows a parallel packing, where the Cu ··· Cu* distance is 3.455(1) Å for (**1**) and 3.624(1) Å for (**2**), respectively.

Imidazolate-bridged Binuclear Copper(II) *Complexes* (**3**) *and* (**4**).—A number of imidazolate-bridged bi- and poly-nuclear copper(II) complexes have been synthesized and characterized.[3] However, in most cases the co-ordination geometries around

the copper(II) ions are identical. The synthetic route for model compounds of besod which satisfy the structural characteristics (i)—(iii) has not been established, although several complexes were synthesized.[4,19] Our synthetic strategy is as follows. A copper(II) complex with an unsymmetrical quadridentate ligand involving an imidazole moiety (a-site component complex) is reacted with a metal complex involving an unsaturated coordination site (b-site component complex) in the presence of alkali to give an imidazolate-bridged binuclear complex satisfying the structural characteristics.

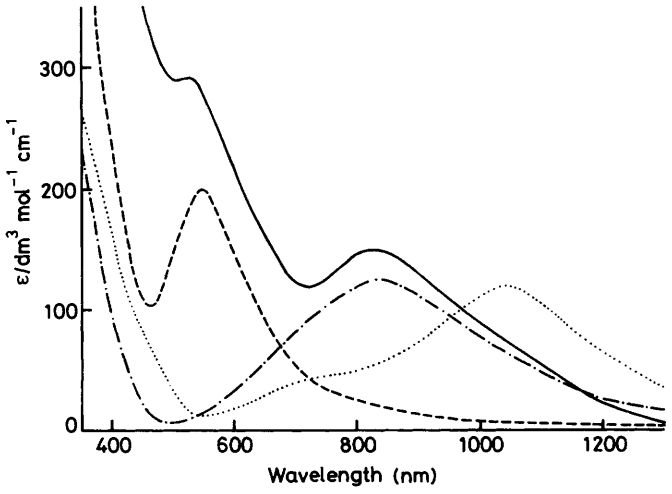

Figure 5. Electronic absorption spectra (in MeCN) of $[Cu(L^1)Cu(tebima)][PF_6][ClO_4]\cdot Me_2CO$ (**4**) (——), the component complexes $[Cu(HL^1)][ClO_4]$ (**1**) (– – –), and $[Cu(tebima)][ClO_4]_2\cdot 2H_2O$ (· · · · ·), and the reference complex $[Cu(tebima)(mim)][ClO_4]_2$ (—·—)

In this study, complex (**1**) was used as the a-site component complex, and $[Cu(tfacac)_2]$ and $[Cu(tebima)][ClO_4]_2\cdot 2H_2O$ were adopted as the b-site component complexes, leading to (**3**) and (**4**).

Electrical conductivity in solution. The molar electrical conductivity of (**3**) measured in chloroform solution is essentially zero, while that of the component complex (**1**) is 94.2 S cm^2 mol^{-1} in methanol and that of $[Cu(tfacac)_2]$ is 0.4 S cm^2 mol^{-1} in chloroform. This means that the imidazole proton of the a-site component complex $[Cu(HL^1)]^+$ is deprotonated to give the neutral complex $[Cu(L^1)]$ which then functions as the ligand at the imidazolate nitrogen to the copper(II) ion of the b-site component complex. The molar electrical conductivity of (**4**) is 300 S cm^2 mol^{-1} in acetone solution which is as expected for 2:1 electrolyte (200—300 S cm^2 mol^{-1}),[17] being consistent with the formula $[Cu(L^1)Cu(tebima)]^{2+}$.

Infrared spectra. The deprotonation of the imidazole proton in the complexes (**3**) and (**4**) is detectable by the i.r. spectra. The ν(N–H) imidazole stretching vibration, which is observed at 3 300 cm^{-1} in the spectrum of the a-site component complex (**1**), disappears in those of (**3**) and (**4**). In addition, the characteristic band due to perchlorate anion (*ca.* 1 100 cm^{-1}) is also absent in (**3**).

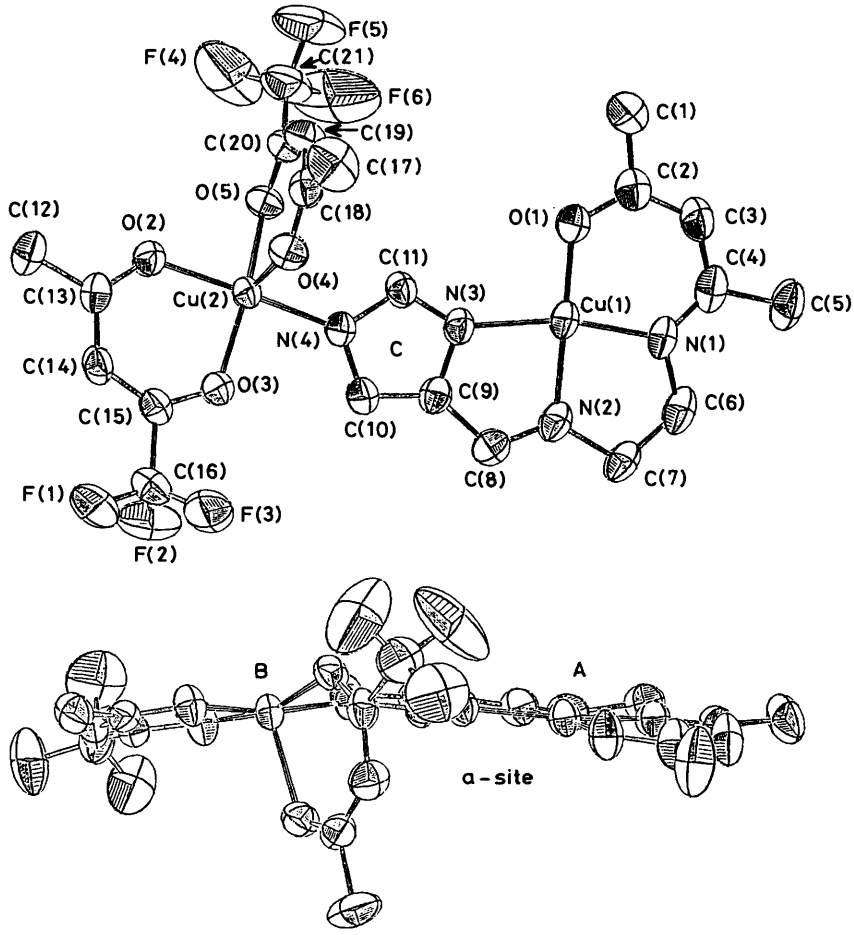

Figure 6. Perspective views of $[Cu(L^1)Cu(tfacac)_2]$ (**3**) with the atom numbering scheme. The hydrogen atoms have been omitted for clarity

Table 9. Relevant bond distances (Å) and angles (°) for the cation of $[Cu(L^1)Cu(tebima)][PF_6][ClO_4]\cdot Me_2CO$ (**4**)

a-Site							
Cu(1)–O	1.864(10)	N(3)–C(11)	1.327(13)	N(1)–C(4)	1.296(16)	C(3)–C(4)	1.399(23)
Cu(1)–N(1)	1.909(9)	N(4)–C(10)	1.363(16)	N(1)–C(6)	1.477(19)	C(4)–C(5)	1.545(19)
Cu(1)–N(2)	1.948(11)	N(4)–C(11)	1.337(13)	N(2)–C(7)	1.464(15)	C(6)–C(7)	1.487(20)
Cu(1)–N(3)	1.963(7)	C(1)–C(2)	1.494(23)	N(2)–C(8)	1.251(14)	C(8)–C(9)	1.450(16)
O–C(2)	1.282(13)	C(2)–C(3)	1.392(19)	N(3)–C(9)	1.389(16)	C(9)–C(10)	1.357(14)
b-Site							
Cu(2)–N(4)	1.957(8)	N(9)–C(29)	1.393(18)	N(7)–C(20)	1.462(18)	N(11)–C(33)	1.346(13)
Cu(2)–N(5)	2.151(9)	N(9)–C(30)	1.488(15)	C(12)–C(13)	1.468(13)	N(11)–C(39)	1.380(16)
Cu(2)–N(6)	1.992(10)	C(22)–C(23)	1.469(21)	C(14)–C(15)	1.406(14)	N(11)–C(40)	1.459(13)
Cu(2)–N(8)	1.968(8)	C(24)–C(25)	1.392(18)	C(14)–C(19)	1.387(19)	C(32)–C(33)	1.483(17)
Cu(2)–N(10)	2.182(8)	C(24)–C(29)	1.405(14)	C(15)–C(16)	1.360(19)	C(34)–C(35)	1.374(16)
N(5)–C(12)	1.511(18)	C(25)–C(26)	1.370(18)	C(16)–C(17)	1.390(22)	C(34)–C(39)	1.415(14)
N(5)–C(22)	1.487(15)	C(26)–C(27)	1.422(17)	C(17)–C(18)	1.396(17)	C(35)–C(36)	1.386(19)
N(5)–C(32)	1.498(14)	C(27)–C(28)	1.348(23)	C(18)–C(19)	1.381(15)	C(36)–C(37)	1.407(17)
N(6)–C(13)	1.318(16)	C(28)–C(29)	1.371(19)	C(20)–C(21)	1.509(18)	C(37)–C(38)	1.349(21)
N(6)–C(14)	1.405(12)	C(30)–C(31)	1.419(29)	N(8)–C(23)	1.333(15)	C(38)–C(39)	1.370(18)
N(7)–C(13)	1.333(16)	N(10)–C(33)	1.337(12)	N(8)–C(24)	1.388(16)	C(40)–C(41)	1.497(22)
N(7)–C(19)	1.384(11)	N(10)–C(34)	1.412(15)	N(9)–C(23)	1.338(15)		
a-Site							
O–Cu(1)–N(1)	97.4(4)	Cu(2)–N(4)–C(11)	121.1(8)	C(4)–N(1)–C(6)	122.7(11)	N(1)–C(6)–C(7)	111.2(11)
O–Cu(1)–N(2)	175.3(4)	C(10)–N(4)–C(11)	106.2(8)	Cu(1)–N(2)–C(7)	114.3(8)	N(2)–C(7)–C(6)	110.5(11)
O–Cu(1)–N(3)	97.0(3)	O–C(2)–C(1)	114.1(11)	Cu(1)–N(2)–C(8)	118.0(8)	N(2)–C(8)–C(9)	114.6(11)
N(1)–Cu(1)–N(2)	84.6(4)	O–C(2)–C(3)	125.4(14)	C(7)–N(2)–C(8)	127.5(12)	N(3)–C(9)–C(8)	114.0(9)
N(1)–Cu(1)–N(3)	165.4(4)	C(1)–C(2)–C(3)	120.3(11)	Cu(1)–N(3)–C(9)	112.1(7)	N(3)–C(9)–C(10)	109.1(10)
N(2)–Cu(1)–N(3)	81.0(4)	C(2)–C(3)–C(4)	125.2(12)	Cu(1)–N(3)–C(11)	143.5(8)	C(8)–C(9)–C(10)	136.7(12)
Cu(1)–O–C(2)	123.9(9)	N(1)–C(4)–C(3)	125.2(11)	C(9)–N(3)–C(11)	104.2(8)	N(4)–C(10)–C(9)	107.4(10)
Cu(1)–N(1)–C(4)	122.4(9)	N(1)–C(4)–C(5)	119.4(13)	Cu(2)–N(4)–C(10)	132.5(7)	N(3)–C(11)–N(4)	112.9(10)
Cu(1)–N(1)–C(6)	114.5(7)	C(3)–C(4)–C(5)	115.3(11)				
b-Site							
N(4)–Cu(2)–N(5)	166.7(3)	C(15)–C(14)–C(19)	120.8(10)	C(13)–N(7)–C(20)	128.6(8)	N(9)–C(29)–C(24)	104.5(10)
N(4)–Cu(2)–N(6)	97.2(3)	C(14)–C(15)–C(16)	116.4(13)	C(19)–N(7)–C(20)	123.9(9)	N(9)–C(29)–C(28)	132.6(10)
N(4)–Cu(2)–N(8)	93.5(3)	C(15)–C(16)–C(17)	122.5(11)	Cu(2)–N(8)–C(23)	113.9(8)	C(24)–C(29)–C(28)	122.7(12)
N(4)–Cu(2)–N(10)	114.1(3)	C(16)–C(17)–C(18)	121.9(10)	Cu(2)–N(8)–C(24)	141.2(7)	N(9)–C(30)–C(31)	112.4(11)
N(5)–Cu(2)–N(6)	81.7(3)	C(17)–C(18)–C(19)	115.3(13)	C(23)–N(8)–C(24)	104.8(9)	N(5)–C(32)–C(33)	108.5(7)
N(5)–Cu(2)–N(8)	80.0(3)	N(7)–C(19)–C(14)	105.9(9)	C(23)–N(9)–C(29)	107.8(9)	N(10)–C(33)–N(11)	113.4(10)
N(5)–Cu(2)–N(10)	78.9(3)	N(7)–C(19)–C(18)	131.1(12)	C(23)–N(9)–C(20)	128.1(12)	N(10)–C(33)–C(34)	122.8(9)
N(6)–Cu(2)–N(8)	143.7(4)	C(14)–C(19)–C(18)	122.9(10)	C(29)–N(9)–C(30)	123.9(11)	N(11)–C(33)–C(34)	123.6(9)
N(6)–Cu(2)–N(10)	98.9(3)	N(7)–C(20)–C(21)	111.7(12)	Cu(2)–N(10)–C(33)	109.9(7)	N(10)–C(34)–C(35)	130.0(9)
N(8)–Cu(2)–N(10)	107.9(3)	N(5)–C(22)–C(23)	106.2(10)	Cu(2)–N(10)–C(34)	145.5(6)	N(10)–C(34)–C(39)	108.7(10)
Cu(2)–N(5)–C(12)	110.0(5)	N(8)–C(23)–N(9)	112.9(12)	C(33)–N(10)–C(34)	104.3(8)	C(35)–C(34)–C(39)	121.1(11)
Cu(2)–N(5)–C(22)	104.8(6)	N(8)–C(23)–C(22)	119.8(10)	C(33)–N(11)–C(39)	107.6(8)	C(34)–C(35)–C(36)	116.3(10)
Cu(2)–N(5)–C(32)	109.1(7)	N(9)–C(23)–C(22)	127.2(10)	C(33)–N(11)–C(40)	127.0(9)	C(35)–C(36)–C(37)	121.1(12)
C(12)–N(5)–C(22)	113.5(10)	N(8)–C(24)–C(25)	130.9(9)	C(39)–N(11)–C(40)	124.6(10)	C(36)–C(37)–C(38)	122.6(13)
C(12)–N(5)–C(32)	111.1(9)	N(8)–C(24)–C(29)	109.9(10)	N(5)–C(12)–C(13)	109.5(10)	C(37)–C(38)–C(39)	116.6(10)
C(22)–N(5)–C(32)	107.9(8)	C(25)–C(24)–C(29)	119.1(11)	N(6)–C(13)–N(7)	113.0(8)	N(11)–C(39)–C(34)	105.7(10)
Cu(2)–N(6)–C(13)	115.1(6)	C(24)–C(25)–C(26)	118.1(10)	N(6)–C(13)–C(12)	123.1(12)	N(11)–C(39)–C(38)	132.3(10)
Cu(2)–N(6)–C(14)	139.4(8)	C(25)–C(26)–C(27)	121.0(13)	N(7)–C(13)–C(12)	123.7(11)	C(34)–C(39)–C(38)	121.9(11)
C(13)–N(6)–C(14)	105.1(10)	C(26)–C(27)–C(28)	121.0(13)	N(6)–C(14)–C(15)	130.6(12)	N(11)–C(40)–C(41)	109.6(12)
C(13)–N(7)–C(19)	107.3(10)	C(27)–C(28)–C(29)	117.8(11)	N(6)–C(14)–C(19)	108.4(8)		

Table 10. Magnetic coupling constants and structural parameters for imidazolate-bridged copper(II) complexes

Complex[a]	$-2J/cm^{-1}$	α_1[b]	α_2[b]	θ_1[b]	θ_2[b]	Ref.
$[Cu_2(bpim)]^{3+}$	163	176.2	171.1	4.7	13.4	24
$[Cu_3(im)_2(Him)_8][ClO_4]_4$	117	162.9	160.9	70.0	60.0	25
$[CuCl(im)(Him)_2]$	84	169.4	168.8	90.0	90.0	23, 26
$[Cu_2(tmdt)_2(im)(ClO_4)_2]^+$	52	161.9	160.2	91.8	90.0	21
$[Cu_2(im)L]^{3+}$	42	158.9	166.3	68.8	79.1	27
$[Cu_2(glyglyO)_2(im)]^-$	38	157.7	157.2	5.8	10.4	*c*
(**3**)	112	176.4	156.6	0.7	22.0	*d*
(**4**)	140	176.9	154.6	0.7		*d*

[a] bpim = 4,5-bis{2-[(2-pyridyl)ethyl]iminomethyl}imidazolate, tmdt = *NNN'N'*-tetramethyldiethylenetriamine, L = 30-membered macrocyclic ligand prepared from 2,6-diacetylpyridine and 3,6-dioxaoctane-1,8-diamine, glyglyO = glycylglycinate(2−), im = imidazolate. [b] The subscripts 1 and 2 refer to two copper atoms in the imidazolate-bridged binuclear unit. [c] K. Matsumoto, S. Ooi, Y. Nakao, W. Mori, and A. Nakahara, *J. Chem. Soc., Dalton Trans.*, 1981, 2045. [d] This work.

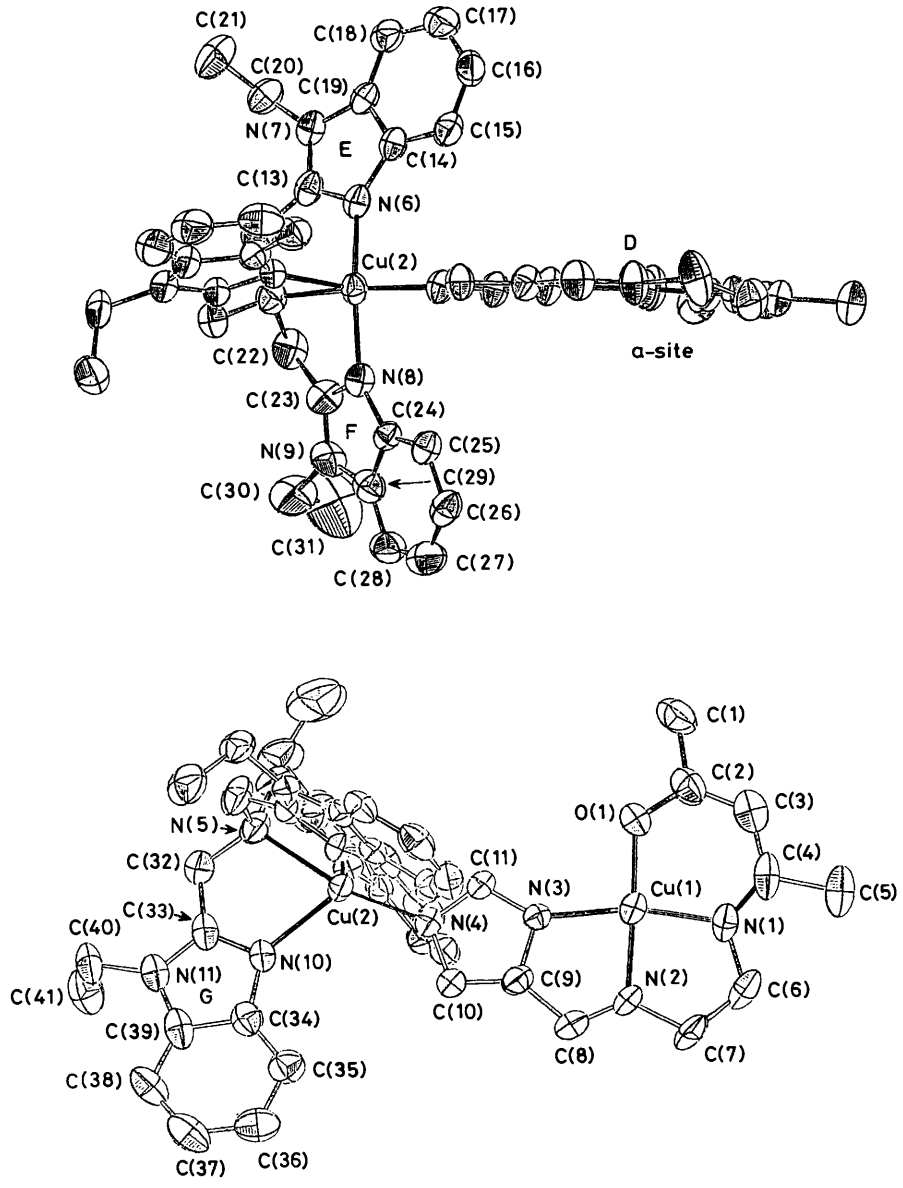

Figure 7. Perspective views of $[Cu(L^1)Cu(tebima)]^{2+}$ (**4**) with the atom numbering scheme. The hydrogen atoms have been omitted for clarity

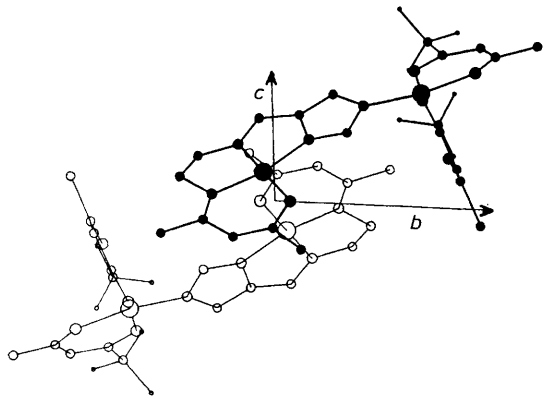

Figure 8. Crystal structure of $[Cu(L^1)Cu(tfacac)_2]$ (**3**) projected on the *a* axis

Electronic spectra. The electronic spectrum of complex (**3**) in acetone exhibits a broad band at 540 nm with an absorption coefficient of 260 $dm^3\ mol^{-1}\ cm^{-1}$ due to a *d–d* transition of the a-site copper(II) sphere, because the spectrum of the a-site component complex (**1**) exhibits a broad band at 550 nm in acetone. The b-site component complex $[Cu(tfacac)_2]$ exhibits two absorptions at 566 (ε 25) and 680 nm (ε 35 $dm^3\ mol^{-1}\ cm^{-1}$) in the visible region.[9] Since the absorption coefficients of the b-site copper(II) complex are small in comparison with those of the a-site component complex, detailed information about the b-site geometry of (**3**) cannot be obtained from the spectrum.

The electronic spectrum of complex (**4**), along with those of the component and reference complexes (**1**), $[Cu(tebima)][ClO_4]_2 \cdot 2H_2O$, and $[Cu(tebima)(mim)][ClO_4]_2$ are shown in Figure 5, where all the spectra were measured in acetonitrile. Complex (**4**) exhibits a shoulder at 530 nm (ε 290 $dm^3\ mol^{-1}\ cm^{-1}$) and a broad band at 835 nm (ε 150 $dm^3\ mol^{-1}\ cm^{-1}$) both

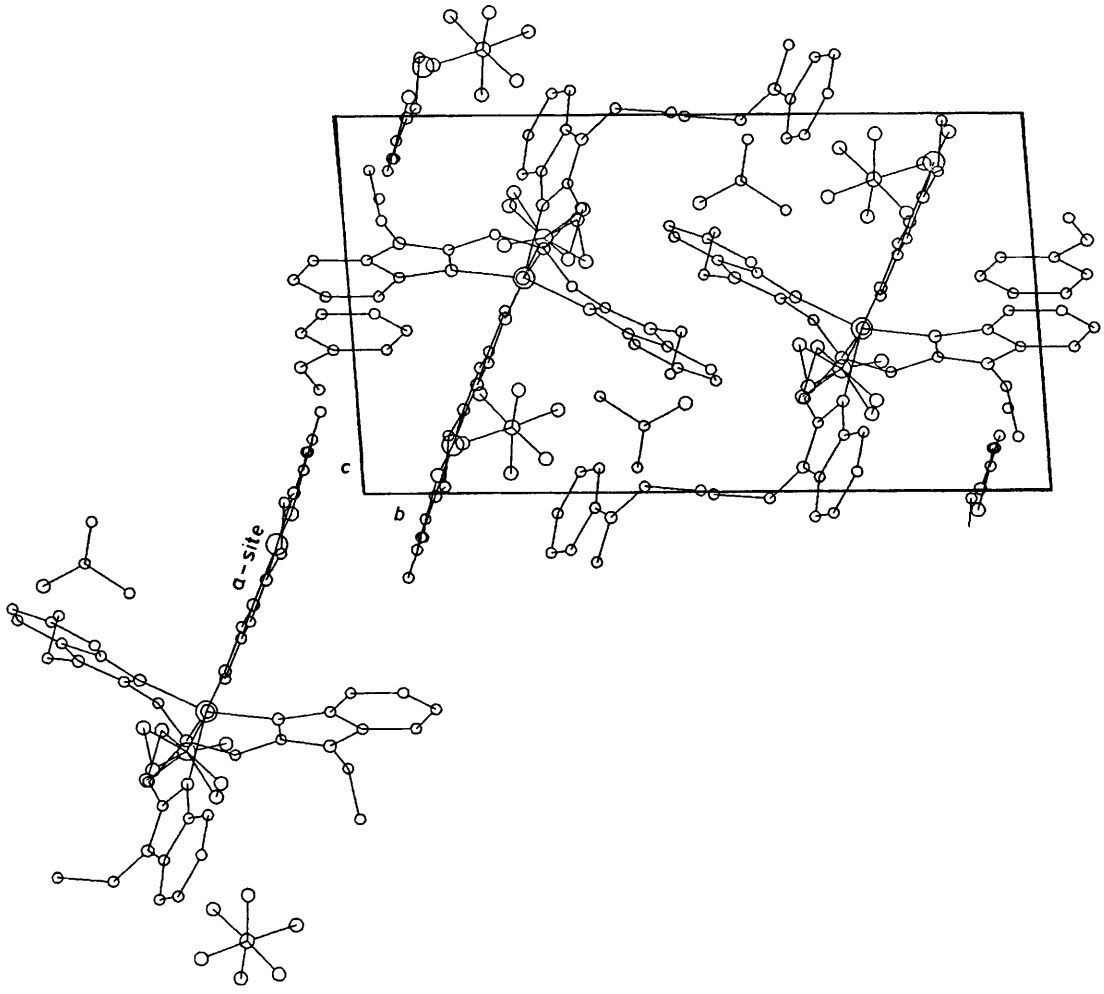

Figure 9. Crystal structure of $[Cu(L^1)Cu(tebima)][PF_6][ClO_4]\cdot Me_2CO$ (**4**) projected on the *a* axis

of which are assigned to *d–d* transitions. The former can be attributed to a *d–d* transition of the a-site copper(II) sphere, because the spectrum of the a-site component complex (**1**) exhibits a band at 550 nm (ε 200 dm^3 mol^{-1} cm^{-1}). The absorption at 835 nm can be attributed to the b-site copper(II) sphere, because the reference complex $[Cu(tebima)(mim)][ClO_4]_2$ exhibits a broad band at 845 nm (ε 125 dm^3 mol^{-1} cm^{-1}). The absorption at 835 nm in (**4**) is indicative of co-ordination of the imidazolate nitrogen of the a-site component to the b-site copper(II) ion, because the absorption at 1 505 nm of the b-site component complex $[Cu(tebima)][ClO_4]_2\cdot 2H_2O$ shifts to shorter wavelength (845 nm) on co-ordination of *N*-methylimidazole in the complex $[Cu(tebima)(mim)][ClO_4]_2$. Therefore the absorption at 835 nm in (**4**) is indicative of the formation of an imidazolate-bridged structure.

Structures of Complexes (**3**) *and* (**4**).—Perspective views of (**3**) and $[Cu(L^1)Cu(tebima)]^{2+}$ (**4**) with the atom numbering schemes are shown in Figures 6—9; bond distances and angles are given in Tables 8 and 9.

$[Cu(L^1)Cu(tfacac)_2]$ (**3**). The *X*-ray analysis has confirmed that (**3**) has a discrete imidazolate-bridged binuclear structure and the co-ordination geometries around the two copper ions are non-identical. The copper(II) ion of the a-site assumes a square-planar co-ordination geometry in which one oxygen atom and three nitrogen atoms of the unsymmetrical quadridentate ligand co-ordinate to the copper(II) ion. The co-ordination plane of the a-site (A) is planar with the largest deviation from the mean plane being 0.06 Å. The saturated five-membered chelate ring has a *gauche* conformation as observed in (**1**). Comparing the bond distances and angles of the imidazolate moiety of (**3**) with those of the imidazole moiety (**1**), the angles N(3)–C(11)–N(4) and C(9)–C(10)–N(4) are larger in (**3**) than the corresponding values in the component complex (**1**) whereas the angle C(10)–N(4)–C(11) is smaller.

The copper(II) ion of the b-site sphere is five-co-ordinate with an imidazolate nitrogen atom N(4) of the a-site ligand and four oxygen atoms of two trifluoroacetylacetonate ligands. This co-ordination geometry can be analysed and described by using an approach developed by Muetterties and Guggenberger.[20] Using this method, the important dihedral angles (known as the 'shape-determining angles,' e_1, e_2, e_3) can be calculated in order to describe a complex geometry. The two possible limiting geometries for a five-co-ordinate metal centre are square-based pyramidal (s.p.) and trigonal bipyramidal (t.b.p.). The angles e_1, e_2, e_3 = 75.7, 75.7, 0° for an s.p. complex and 53.1, 53.1, 53.1° for a t.b.p. complex. Applied to the b-site sphere, the analysis yields the parameters 79.1, 79.0, 6.9°. Thus, the co-ordination geometry can be best described as slightly distorted s.p., where the basal plane (B) comprises an imidazolate nitrogen atom N(4) and three oxygen atoms of trifluoroacetylacetonate ligands [O(2), O(3), and O(5)], and the axial position is

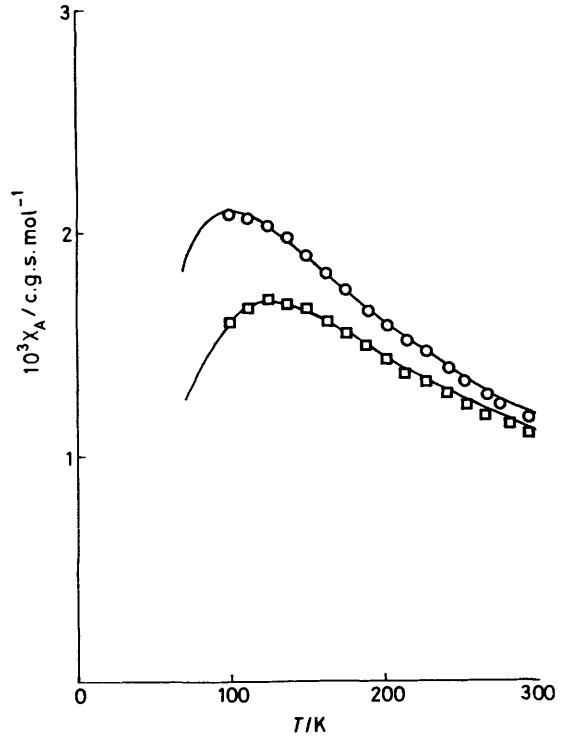

Figure 10. Temperature dependences of the magnetic susceptibilities of $[Cu(L^1)Cu(tfacac)_2]$ (**3**) (○) and $[Cu(L^1)Cu(tebima)][PF_6][ClO_4]\cdot Me_2CO$ (**4**) (□). The solid curves represent theoretical values

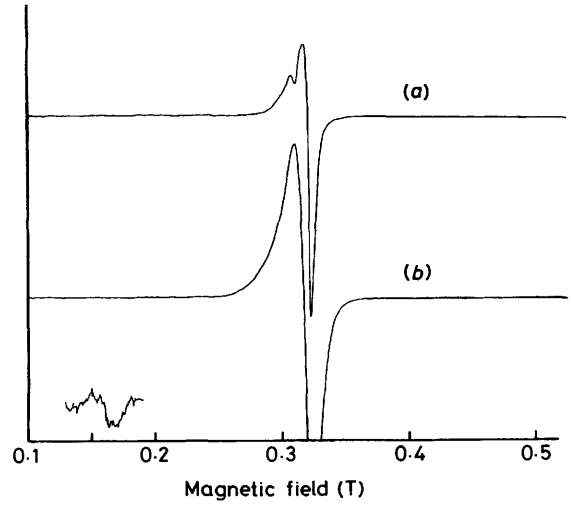

Figure 11. E.s.r. spectra of (**3**) at *X*-band frequency and 77 K: (*a*) polycrystalline powder, (*b*) in chloroform

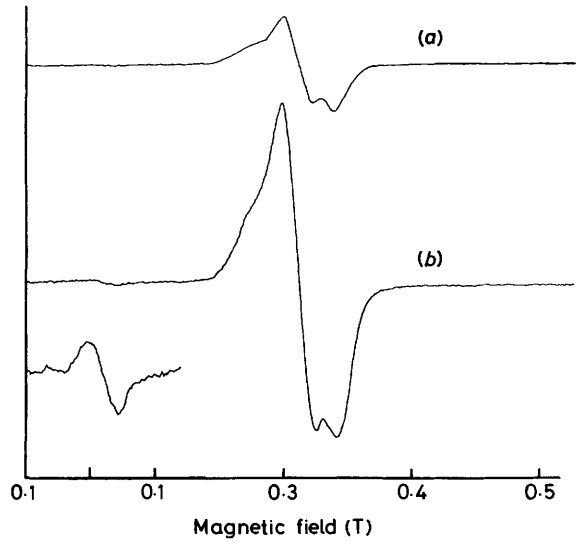

Figure 12. E.s.r. spectra of (**4**) at *X*-band frequency and 77 K: (*a*) polycrystalline powder, (*b*) in acetonitrile

occupied by O(4). The basal plane (B) is planar within a deviation of 0.06 Å and the copper atom Cu(2) deviates 0.20 Å toward the axial ligand O(4). The dihedral angle between two trifluoroacetylacetonate chelate rings is 86.8°, where each chelate ring is planar, the largest deviation from the mean plane being 0.005 Å. Since it is known that the b-site component complex $[Cu(tfacac)_2]$ assumes a square-planar four-co-ordinate geometry,[9] it is found that a structural rearrangement with respect to two trifluoroacetylacetonate ligands has occurred by the co-ordination of the imidazolate nitrogen atom to the b-site copper(II) ion in (**3**).

The Cu(2)–N(4) (imidazolate nitrogen) distance of 1.966(3) Å is within the range of values normally found for this type of bond.[2] The bridging imidazolate ring is planar with the largest deviation from the mean plane being 0.003 Å. The copper atoms Cu(1) and Cu(2) deviate 0.07 and 0.20 Å from the plane on the same side. The co-planarity among the imidazolate ring (C), the co-ordination plane of the a-site (A), and the basal co-ordination plane of the b-site (B) was examined from their dihedral angles. The angle between A and C is 0.7° and the angle between B and C is 22.0°. Thus, the imidazolate-bridged binuclear complex (**3**) is 'bowed' as shown in Figure 6.

The parallel packing between the a-site complex with planar geometry and the symmetry-related complex $(-x + 2, -y, -z)$ is observed, where the Cu(1) ··· Cu(1′) distance is 3.621(1) Å. The intra-molecular Cu(1) ··· Cu(2) distance is 5.996(3) Å.

$[Cu(L^1)Cu(tebima)][PF_6][ClO_4]\cdot Me_2CO$ (**4**). The crystal structure consists of discrete imidazolate-bridged binuclear cations $[Cu(L^1)Cu(tebima)]^{2+}$, PF_6^- and ClO_4^- anions, and acetone as crystal solvent. In the imidazolate-bridged binuclear cation, the co-ordination geometries around the two copper(II) ions are non-identical. The copper(II) ion of the a-site sphere assumes a square-planar co-ordination geometry as observed in (**3**) and the component complex (**1**). The angles in the imidazolate moiety show a similar feature to that observed in (**3**), when they are compared to the angles of the imidazole moiety of the component complex (**1**).

The b-site sphere is five-co-ordinate with one tertiary amine nitrogen and three benzimidazole nitrogen atoms of the tripodal ligand tebima and one imidazolate nitrogen atom of the a-site ligand. The co-ordination geometry was analysed by the method of Muetterties and Guggenberger.[20] The analysis yields the shape-determining parameters e_1, e_2, e_3 = 72.0, 63.7, 18.5°. Thus, the co-ordination geometry of the b-site sphere is intermediate between s.p. and t.b.p.

The Cu(2)–N(4) (imidazolate nitrogen) bond distance of 1.957(8) Å is the shortest of the five Cu(2)–N bond distances of the b-site sphere. The Cu(2)–N(4) bond distance is within the range normally found for this bond.[21] Of three Cu(2)–N (benzimidazole nitrogen) bond distances, Cu(2)–N(10) [2.182(8) Å] is longer than the other two Cu(2)–N(6) [1.992(10) Å] and Cu(2)–N(8) [1.968(8) Å]. The dihedral angles between the a-site

co-ordination plane (D) and each of three benzimidazole rings (E, F, and G, see Figure 7) are 103.0 (−77.0), 78.1, and 18.7°, respectively. The bridging imidazolate ring is planar, the largest deviation being 0.003 Å; the deviations of the atoms Cu(1), Cu(2), N(5), N(6), N(8), and N(10) are −0.03, 0.16, 0.36, −1.69, 2.06, and −0.01 Å, respectively.

The parallel packing between the a-site complex with a planar geometry and the symmetry-related complex $(-x, -y, -z)$ is observed, where the Cu(1) ··· Cu(1′) distance is 5.351(3) Å.The intra-molecular Cu(1) ··· Cu(2) distance is 5.996(3) Å.

Magnetic Properties of (**3**) *and* (**4**).—Temperature dependences of the magnetic susceptibilities for complexes (**3**) and (**4**) are shown in Figure 10. The magnetic susceptibility data were analysed on the basis of the Bleaney-Bowers equation (1) for

$$\chi_A = \frac{Ng^2\beta^2}{kT}\left[\frac{1}{3 + \exp(-2J/kT)}\right] + N\alpha \qquad (1)$$

isotropic exchange in a copper(II) dimer, using the Heisenberg spin Hamiltonian of the form $\hat{\mathcal{H}} = -2J\hat{S}_1\cdot\hat{S}_2$ where the symbols have their usual meanings and the temperature-independent paramagnetism ($N\alpha$) is taken to be 60×10^{-6} c.g.s. mol^{-1}. The best-fit parameters are $g = 2.12$ and $2J = -112$ cm^{-1} for complex (**3**) and $g = 2.12$ and $2J = -140$ cm^{-1} for complex (**4**). The generalized R factor, $R = \{\Sigma[\chi_A(\text{obs.}) - \chi_A(\text{calc.})]^2/\Sigma\chi_A(\text{obs.})^2\}^{\frac{1}{2}}$, a convenient statistical indicator of the quality of the fits, was 0.008 for (**3**) and 0.020 for (**4**). In Figure 10, theoretical curves with the parameters of g and J obtained are shown as solid lines. The antiferromagnetic interaction parameters ($2J$) obtained are fairly large compared with the values for the imidazolate-bridged polynuclear copper(II) complexes so far reported (Table 10).

The X-band e.s.r. spectra of complexes (**3**) and (**4**) were measured in polycrystalline powder and in solution at ambient and liquid-nitrogen temperatures. The spectra of (**3**) in polycrystalline powder and in chloroform at 77 K are shown in Figure 11. The spectra of (**4**) in polycrystalline powder and in acetonitrile at 77 K are shown in Figure 12. The spectra of the powder samples of (**3**) and (**4**) at 77 K show a broad signal at $g = 2.06$ for (**3**) and $g = 2.08$ for (**4**) assignable to the $\Delta M = 1$ transition, while the $\Delta M = 2$ transition was not observed under the present conditions. The broadening of the $\Delta M = 1$ signal is a feature expected for a spin-coupled copper(II) dimer. The frozen solution samples of (**3**) and (**4**) at 77 K give similar spectra comprising two features of very different intensities. In both cases, a $\Delta M = 1$ signal appears as a broad signal and a much weaker signal is observed at 'half-field' which is recognised as a $\Delta M = 2$ transition.[22] The appearance of the $\Delta M = 2$ signal indicates that an imidazolate-bridged binuclear structure exists even in solution, as predicted by the electronic absorption spectra in solution.

Correlation between magnetic coupling and structural parameters. Recently Bencini *et al.*[23] have examined the mechanism of the exchange interaction between two copper(II) ions bridged by an imidazolate ligand using the extended Hückel molecular orbital method and concluded that the extent of the coupling depends predominantly on the structural parameters α (the angle between Cu–N and N–N vectors) and θ [the dihedral angle between the plane of the magnetic orbital on the copper(II) ions and the imidazolate plane]. The structural parameters (α and θ) and the magnetic coupling constants of the complexes (**3**) and (**4**), along with those of the complexes reported already, are given in Table 10. Reflecting the non-identical co-ordination geometries in the binuclear unit, the structural parameters α_1 and α_2 of (**3**) and (**4**) are quite different from each other. The structural parameter α_1 referred to the a-site sphere of (**3**) agrees well with that of (**4**), as expected on the basis that the imidazolate moiety is incorporated in the quadridentate chelate ligand and the structure of the a-site sphere is rigid. The parameters α_1 of (**3**) and (**4**) are the largest values reported so far, while the parameters α_2 referred to the b-site sphere are the smallest. At this stage, a rationalisation of the fairly large coupling constant (large α_1) and small α_2 angles seems difficult by the simple application of the analysis of Bencini *et al.*[23] However, we believe that the present data give a general understanding of the relationship between the magnetic coupling constant and structural parameters, and are a useful basis for further studies.

Conclusions

Two imidazolate-bridged binuclear copper(II) complexes $[Cu(L^1)Cu(tfacac)_2]$ (**3**) and $[Cu(L^1)Cu(tebima)][PF_6]$-$[ClO_4]\cdot Me_2CO$ (**4**) with non-identical co-ordination geometries in their binuclear units have been prepared by the reaction of a copper(II) complex with an unsymmetrical quadridentate ligand involving an imidazole moiety (a-site component complex) and $[Cu(tfacac)_2]$ or $[Cu(tebima)][ClO_4]_2\cdot 2H_2O$ containing an unsaturated co-ordination site (b-site component complex) in the presence of triethylamine. The deprotonated a-site component complex $[Cu(L^1)]$ which can function as a ligand at the imidazolate nitrogen has been isolated. The complex is very effective in the synthesis of the imidazolate-bridged polynuclear complex. The X-ray structural analyses of (**3**) and (**4**) verified the detailed structures. Analyses of the magnetic susceptibilities gave the antiferromagnetic coupling constants $2J = -112$ cm^{-1} for (**3**) and $2J = -140$ cm^{-1} for (**4**), which are fairly large compared with others reported[22–27] for imidazolate-bridged polynuclear copper(II) complexes. The e.s.r. and electronic spectra measured in solution show that the imidazolate-bridged binuclear structure exists even in solution.

It is expected that the present synthetic procedure can be easily applied to the synthesis of imidazolate-bridged heterometal bi- or poly-nuclear complexes with non-identical co-ordination geometries which may be used as model compounds of besod and cytochrome c oxidase.

Acknowledgements

We wish to thank Professor Sigeo Kida, Faculty of Science, Kyushu University, for use of the X-ray diffractometer and the e.s.r. spectrometer. We are indebted to Mr. Masayuki Koikawa, Kyushu University, for e.s.r. measurements. We also thank the Institute for Molecular Science, Okazaki National Laboratory, for use of the X-ray diffractometer and computer. The support of a Grant-in-Aid for Scientific Research from the Ministry of Education, Science and Culture (Japan) is gratefully acknowledged.

References

1 J. A. Fee, *Biochim. Biophys. Acta*, 1973, **295**, 107; J. S. Richardson, K. A. Thomas, B. H. Rubin, and D. C. Richardson, *Proc. Natl. Acad. Sci. USA*, 1975, **72**, 1349.

2 G. Palmer, G. T. Babcock, and L. E. Vickery, *Proc. Natl. Acad. Sci. USA*, 1976, **73**, 2206.

3 C. O'Young, J. C. Dewan, H. R. Lilienthal, and S. J. Lippard, *J. Am. Chem. Soc.*, 1978, **100**, 7291; R. N. Katz, G. Kolks, and S. J. Lippard, *Inorg. Chem.*, 1980, **19**, 3845; G. Kolks, C. R. Frihart, P. K. Coughlin, and S. J. Lippard, *ibid.*, 1981, **20**, 2933; M. Sato, K. Kodama, M. Uehara, and J. Nakaya, *J. Chem. Soc., Chem. Commun.*, 1984, 51; M. Suzuki, H. Kanatomi, H. Koyama, and I. Murase, *Inorg. Chim. Acta*, 1980, **44**, L41.

4 S. E. Dessens, C. L. Merrill, R. J. Saxton, R. L. Ilaria, J. W. Lindsey, and L. J. Wilson, *J. Am. Chem. Soc.*, 1982, **104**, 4357; T. Prosperi and A. A. G. Tomlinson, *J. Chem. Soc., Chem. Commun.*, 1979, 196; R. J. Saxton and L. J. Wilson, *ibid.*, 1984, 359.

5 J. R. Totten and W. J. Darby, *Org. Synth.*, Wiley, New York, 1955, Col. Vol. III, p. 460.
6 R. A. Turner, C. F. Huebner, and C. R. Scholz, *J. Am. Chem. Soc.*, 1949, **71**, 2802.
7 E. Papadopoluos, A. Jarrar, and C. H. Issidarides, *J. Org. Chem.*, 1966, **31**, 615.
8 J. P. Costes, F. Dahan, and J. P. Laurent, *Inorg. Chem.*, 1985, **24**, 1018; J. P. Costes, G. Cros, M. H. Darbiew, and J. P. Laurent, *Inorg. Chim. Acta*, 1982, **60**, 111.
9 R. L. Belford, A. E. Martel, and M. Calvin, *J. Inorg. Nucl. Chem.*, 1956, **2**, 11.
10 L. K. Thompson, B. S. Ramaswamy, and E. A. Seymour, *Can. J. Chem.*, 1977, **55**, 878.
11 V. McKee, M. Zvagulis, J. V. Dagdigian, M. G. Patch, and C. A. Reed, *J. Am. Chem. Soc.*, 1984, **106**, 4765.
12 M. Mikuriya, H. Ōkawa, and S. Kida, *Bull. Chem. Soc. Jpn.*, 1983, **54**, 2943.
13 T. Sakurai and K. Kobayashi, *Rikagaku Kenkyusho Houkoku*, 1979, **55**, 69; S. Kawano, *Rep. Comput. Cent. Univ. Kyushu*, 1980, **13**, 39.
14 'International Tables for *X*-Ray Crystallography,' Kynoch Press, Birmingham, 1974, vol. 4.
15 R. F. Stewart, E. R. Davidson, and W. T. Simpson, *J. Chem. Phys.*, 1965, **42**, 3175.
16 H. A. Kuska, M. F. Farona, P. Pappas, and S. Potterton, *J. Coord. Chem.*, 1971, **1**, 259; N. Matsumoto, M. Asakawa, H. Nogami, M. Higuchi, and A. Ohyoshi, *J. Chem. Soc., Dalton Trans.*, 1985, 101.
17 W. J. Geary, *Coord. Chem. Rev.*, 1971, **7**, 81.
18 N. Matsumoto, A. Ohyoshi, and H. Ōkawa, unpublished work.
19 J. P. Costes, J. F. Serra, F. Dahan, and J. P. Laurent, *Inorg. Chem.*, 1986, **25**, 2790.
20 E. L. Muetterties and L. J. Guggenberger, *J. Am. Chem. Soc.*, 1974, **96**, 1748.
21 G. Kolks, S. J. Lippard, J. V. Wasczak, and H. R. Lilienthal, *J. Am. Chem. Soc.*, 1982, **104**, 717.
22 H. M. J. Hendriks, P. J. M. W. L. Birker, G. C. Verschoor, and J. Reedijk, *J. Chem. Soc., Dalton Trans.*, 1982, 623; A. Bencini, D. Gatteschi, C. Zanchini, J. G. Haasnoot, R. Prins, and J. Reedijk, *Inorg. Chem.*, 1985, **24**, 2812.
23 A. Bencini, C. Benelli, D. Gatteschi, and C. Zanchini, *Inorg. Chem.*, 1986, **25**, 1748.
24 J. C. Dewan and S. J. Lippard, *Inorg. Chem.*, 1980, **19**, 2079.
25 C. Benelli, R. K. Bunting, D. Gatteschi, and C. Zanchini, *Inorg. Chem.*, 1984, **23**, 3074.
26 B. K. S. Lundberg, *Acta Chem. Scand.*, 1972, **26**, 3902.
27 M. G. B. Drew, M. McCann, and S. M. Nelson, *J. Chem. Soc., Dalton Trans.*, 1981, 1868.

Received 4*th March* 1987; *Paper* 7/405